Life SEDREMED

ENHANCED BIOREMEDIATION OF

CONTAMINATED MARINE SEDIMENTS

LIFE20 ENV/IT/000572

START DATE OF THE PROJECT: 1 October 2021

DURATION OF THE PROJECT: 42 months

DELIVERABLE (B3.1)
First report with monitoring results

DUE DATE OF DELIVERABLE: October 31, 2023

ACTUAL SUBMISSION DATE: May 07, 2024

BENEFICIARIES LEADING THIS DELIVERABLE: UNIVPM, ISO, SZN, INVITALIA

Index

1. Executive Summary

The Monitoring strategy is one of the fundamentals of our Life Project SEDREMED, since the effectiveness of the remediation approaches is closely tied to the monitoring results.
One of the project's objectives is to apply state of art and innovative monitoring tools for assessing the efficacy of the tested technologies in the remediation of contaminated marine sediments of Bagnoli, one of the most polluted sites in Europe, as well as their ecological compatibility.
This first report will provide a description of the sampling campaigns, of the outcomes of the various analyses until now, and of the mesocosm test results.
Based on the findings of the ABBACO Project, preliminary campaigns were conducted to determine which area would be best suited to serve as a pilot area. In order to track the effectiveness of the biodegradation process, BACTRAPS, an innovative device created by Isodetect for the purposes of assess the natural biodegradation that already occurs in situ, were also inserted and subsequently recovered during this phase. Additionally, IDRABEL received surface sediment samples for the mesocosm testing phase.

Following this initial stage, a high-contaminated area (site H) had been selected and a nearby zone was designated as the control area.
Then, the installation began in November 2023, employing a specific configuration that was selected to improve the technology's efficiency.
Some analyses, that began prior to the installation of the in-situ technologies, continued throughout and after it, while other analyses, such as the BACI (Before-After-Control-Impact) approach, will be replicated only after the dismantling of the plant.
Due to the delay in the in-situ installation, the results provided in this deliverable are based on samples taken before the installation and on laboratory experiments. Exhaustive data on the monitoring results will be provided in the final report on the monitoring results (Deliverable B3.2).

Main conclusions of this first analysis are that polyaromatic compounds exhibit natural attenuation, albeit at a modest level. The Bio-Vase product has slightly increased the biodegradation of PAHs and has been shown to adsorb/immobilize heavy metals, as previously assumed. Heavy hydrocarbons (C>12) and PCBs have also been identified as relevant contaminants in the collected sediments. This means that the remediation potential of the tested technology will also be evaluated for these contaminants.

There are no clear results from mesocosms on the remediation efficiency of the EKOGRID technology alone or in combination with the IDRABEL product. The in situ treatment will provide more clear and conclusive outcomes for the effective final remediation.

1. State of art and background

1.1 Challenges of the Bagnoli site

Environmental contamination by polycyclic aromatic hydrocarbons (PAHs) and metals is reaching a global dimension and represents a serious risk for the sustainable provision of ecosystems' goods and services and for human wellbeing (Johnston, 2015). Chemical contamination can impair biological components at different trophic levels, from microbes to top predators (Gupta, 2019 and citations therein). In Europe, environmental contamination is often linked to intense industrial activities, that in many cases, are located near the coast, representing a high ecological risk for both terrestrial and marine environments, even after the end of the industrial exploitation (Armiento, 2020). This issue is widely widespread; indeed, it has been estimated the potential presence of 2.5 million polluted sites, specifically where industrial activities took place (EEA, 2019).

The Bagnoli site, located in the Gulf of Naples (IT), is listed among the Italian contaminated Sites of National Interest (SIN) for the high levels of chemical contamination due to industrial activities, mainly represented by a steel plant using fossil coal, iron and limestone, which began in 1905 and ended at the beginning of nineties when the plant was dismissed. Here, PAH concentrations in the sediment can be three to four orders of magnitude higher than those reported from several marine benthic systems worldwide (Dell'Anno et al., 2020), thus demanding effective and sustainable remediation solutions.

1.2 Advanced remediation technologies

Conventional remediation practices of marine sediments can be highly costly and could cause major ecological impacts. Typically, they are made through mechanical dredging of the contaminated sediments, causing the remobilisation of pollutants. Moreover, the strategies for the management of dredged contaminated sediments, which are typically based on landfill disposal and/or confined aquatic disposal (Bortone et al., 2004), have several disadvantages, such as limited space capacity, high cost, and low environmental sustainability and compatibility (Rulkens, 2005; Akcil et al., 2015; Lofrano et al., 2017). In contrast, *in situ* bioremediation is an environmental-friendly strategy gaining increasing attention for its potential to clean-up hydrocarbon contaminated marine sediments (Akcil et al., 2015; Beolchini et al., 2010; Dell'Anno et al., 2012; Head et al., 2006; Chen et al., 2017; Kronenberg et al., 2017). Different field and laboratory experiments demonstrated that the biodegradation of hydrocarbons in the sediments can be accelerated through the addition of inorganic nutrients and/or different electron acceptors/donors able to stimulate the autochthonous microbial assemblages (Atlas, 1995; Head and Swannell, 1999; Kasai et al., 2002; Head et al., 2006; Atlas and Bragg, 2009; Dell'Anno et al., 2012; Kalantary et al., 2014; Dell'Anno et al., 2020). In this regard, microbial fuel cell-based

strategies employing solid-state electrodes as electron donors or acceptors have been recently proposed to stimulate biodegradation processes in contaminated sediments (Cruz Viggi et al., 2015, 2017; Kronenberg et al., 2017; Nastro et al., 2019). Also, bioaugmentation strategies, based on the addition of specific microbial taxa to enhance biodegradation processes, can be effective for the remediation of sediment contaminated with hydrocarbons (Yu et al., 2005; Jacques et al., 2008), but to date in situ applications are still in infancy and require optimisation. In SEDREMED, these technological approaches are provided by the companies Ekogrid (electrochemical stimulation) and IDRABEL (particle- & bio-augmentation).

The combination of above mentioned *in situ* bioremediation technologies has not been tested yet and this represents the major challenge of the SEDREMED project. Although bioremediation can be effective for removing hydrocarbons, this strategy could induce important changes in the partitioning, mobility and bioavailability of heavy metals in the sediment, possibly increasing environmental risk (Dell'Anno et al., 2009; Rocchetti et al., 2012; Fonti et al., 2015; Dell'Anno et al., 2020). Therefore, an accurate risk analysis should be conducted to assess the contextual effects of the biotreatments on marine sediments characterized by mixed chemical contamination (due to the presence of both organic and inorganic contaminants), as in the case of Bagnoli area.

1.3 Advanced and integrated monitoring tools

Risk assessment, optimization, and monitoring of the performance of remediation technologies require effective tools. In no case, the simple determination of contaminant concentrations and standard environmental parameters will provide adequate information for efficient application of innovative treatments, as their development depends on a deeper understanding of processes such as contaminant degradation, mineralization and sorption/desorption. These processes can be highly complex and variable according to environmental conditions, which are supposed to be triggered to a most favorable state by applied technologies.

In the recent decade, a toolbox of innovative monitoring methods has been developed providing multiple lines and levels of evidence for natural and enhanced attenuation processes of contaminants in groundwater systems (see Figure 1). The SEDREMED challenge is the transfer, and improvement of these tools to coastal marine sediments, which requires specific optimizations and adaptations (e.g. special lancets for BACTRAPS). At the same time, the SEDREMED project will use additional state of art monitoring tools to provide evidence of the eco-compatibility and potential ecological benefits of the selected remediation technologies. Overall, the applied methods will elucidate contaminant degradation (by isotope labelling, metabolite detection, diagnostic ratios, or molecular analyses) and will provide insights on the potential benefits in terms of reduction of ecotoxicological risks (by specific bioassays) and on biodiversity and key ecological attributes. The application of advanced and integrated monitoring

tools should be the benchmark for the successful implementation of remediation technologies not only at Bagnoli site, but at any other contaminated coastal area.

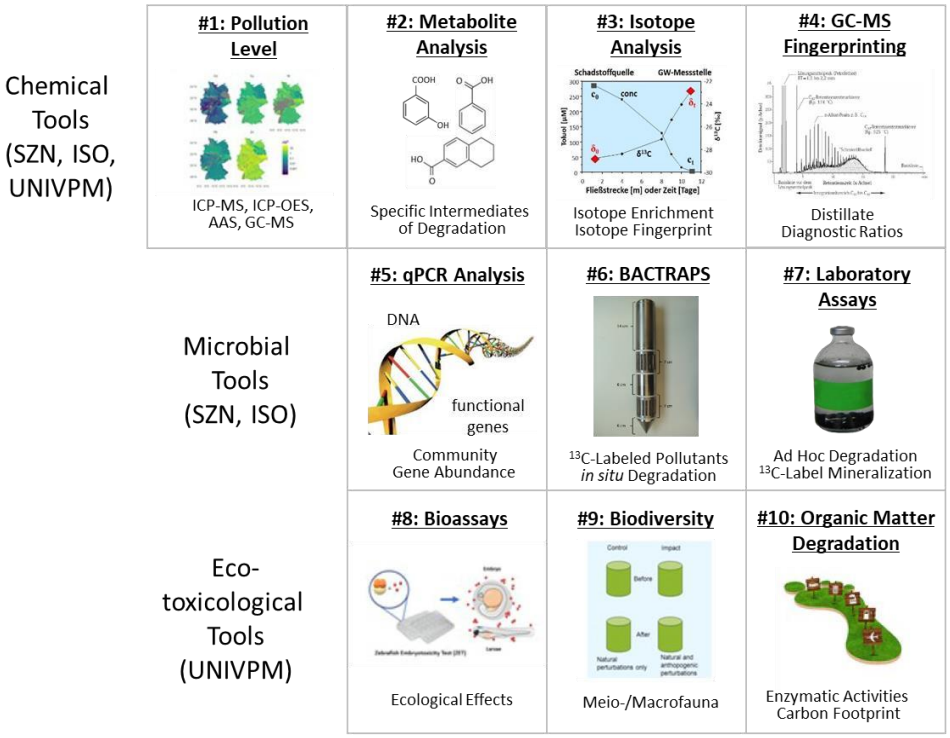

Figure 1. Schematic overview of the monitoring tools for assessing the effectiveness and ecocompatibility of the remediation technologies in SEDREMED.

2. Sampling campaigns

Since the assessment of remediation efficiency and ecological compatibility in contaminated marine sediments is a challenging task, state of art and advanced monitoring tools, properly adapted and improved for coastal marine areas, are applied in the SEDREMED project (Figure 1). In this deliverable related to Action B3 of SEDREMED (D3.1), we provide results on the monitoring performed on the area selected for the *in-situ* application of EKOGRID and IDRABEL technologies as well as on findings of laboratory experimental tests. To select the most suitable area as a pilot

test field, sampling activities were preliminary carried out in July 2022 and then in December 2022 and November 2023.

2.1 Preliminary sampling campaign

For preliminary monitoring analysis, surface sediment samples (the top 20 cm) were collected in July 2022 in an area identified for the in-situ experiments. To this aim, UNIVPM, SZN and ISO discussed and agreed on a sampling strategy and defined the set of variables to be analysed. In particular, surface sediment samples were collected by three independent Van Veen grab deployments in a single site (40°48.350' N, 14°10.020' E) and subsequently analysed for the concentrations of main contaminants previously identified during the ABBACO project, which include metals/metalloids (i.e. Al, As, Ba, Cd, Cr, Fe, Mn, Ni, Pb, Cu and Zn), hydrocarbons C>12 and sixteen different PAHs congeners of priority concern (i.e, naphthalene, acenaphthene, fluorene, acenaphthylene, phenanthrene, anthracene, fluoranthene, pyrene, benzo[a]anthracene, chrysene, benzo[b]fluoranthene, benzo[k]fluoranthene, benzo[a]pyrene, indeno[1,2,3,-cd]pyrene, dibenzo[a,h]anthracene, benzo[g,h,i]perylene), which sum represents the total concentration of PAHs. All these analyses were carried out using state of art methodologies which were previously used on Bagnoli sediments, thus allowing a proper comparison.

Surface sediment samples collected in July 2022 were also used for *ad hoc* laboratory assays which were carried out to monitor over time the bioremediation performance of a new version of BioVase formula developed by IDRABEL. In April and October 2023, SZN collected additional surface sediment samples (the top 20 cm, ca. 100 kg), just as in July 2022, and sent them to IDRABEL to run mesocosm experiments.

2.2 Sampling campaigns for in depth monitoring of the treatment area

A monitoring campaign was conducted by DST (Deep Sea Technology) using specific sampling tool (vibrocoring) in December 2022 at two potential treatment areas, a heavy-contaminated pilot test site H (40°48.349'N; 14°10.020'E) and a low-contaminated pilot test site L (40°48.294'N; 14°10.076'E). In each selected area, two independent sediment cores, down to ca. 170 cm depth, were recovered and sliced into different sediment layers (e.g., 0-50 cm, 50-100 cm, >100 cm). These samples have been analyzed by various monitoring tools and were also used for laboratory assays. Altogether, sediment material was collected from 16 sediment layers (2 sites x 2 cores x 4 sediment depths).

For *in-situ* monitoring of biodegradation performance ISO developed special lancets containing microcosms with labelled (^{13}C & ^{2}H) polycyclic aromatic hydrocarbons (BACTRAPS). BACTRAP lancets were inserted on November 4th, 2022 at two different depths into the sediment (0-15 cm and 2035 cm) of each test field and contained BACTRAPS loaded either with $^{13}C/^{2}H$-

naphthalene or $^{13}C/^{2}H$acenaphthene. All the BACTRAPS were successfully recovered on January 27th 2023, after 83 days of in situ exposition.
According to the results of pre-investigations, the heavy-contaminated pilot test site H close to a pier was selected for treatment with EKOGRID and IDRABEL technologies. In addition, a neighboring area was identified and used as an untreated control area (Figure 2). The technological setup took place in November 2023, and was accompanied by the collection of 6 sediment cores by vibrocoring immediately before. In particular, two sediment cores were collected in the experimental plot in which Ekogrid and IDRABEL technologies will be used in combination, two sediment cores in the experimental plot where only Ekogrid technology will be tested, and two sediment cores in an adjacent untreated area to be used as control (Figure 2).

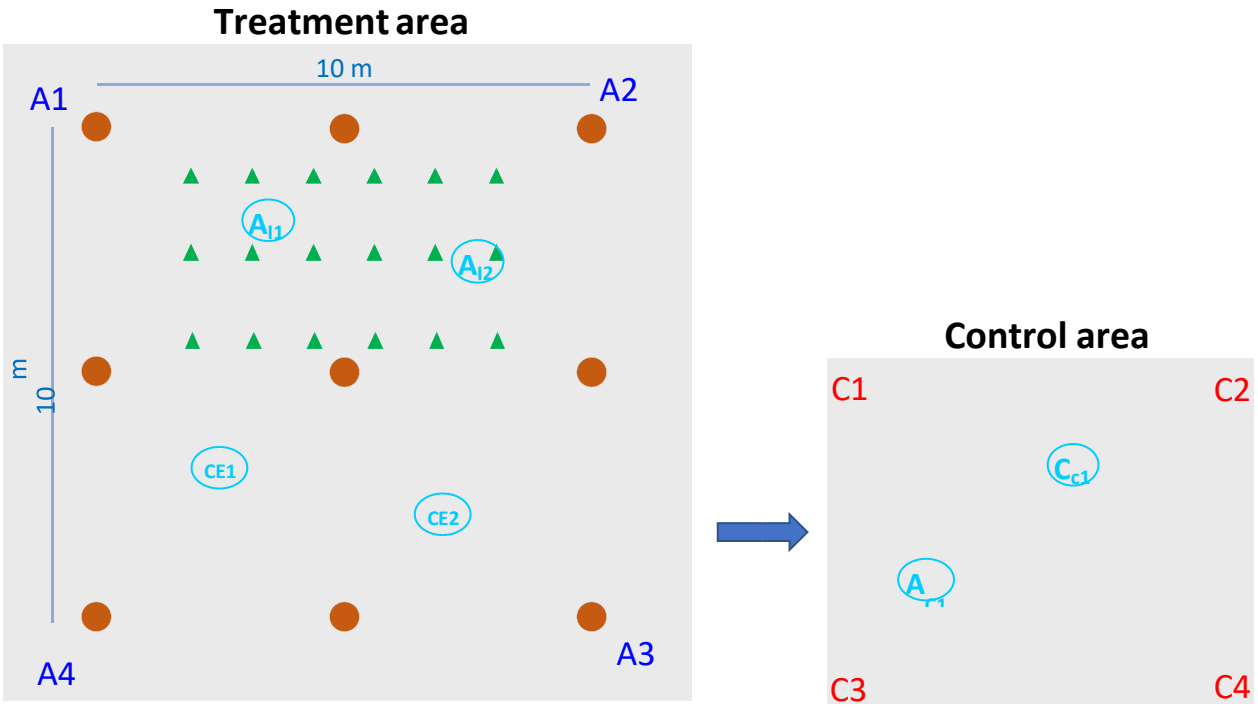

Figure 2. Schematic overview of the sampling locations of the 4 sediment cores in the pilot treatment area (AI1, AI2, CE1, CE2), where EKOGRID electrodes (red circles) and IDRABEL products (green triangles) will be used, and of the 2 sediment cores in the control area (AC1, CC1).

Each core was sliced in three sediment layers (0-50 cm, 50-100 cm, 100-bottom) and sediment subsamples were used for ecotoxicological and chemical analysis. In addition, small amounts of sediments were collected from seven closer layers (0-2 cm, 20 cm, 40 cm, 60 cm, 90 cm, 120 cm, 150 cm/bottom) and preserved in RNA later for molecular analysis (Figure 3).

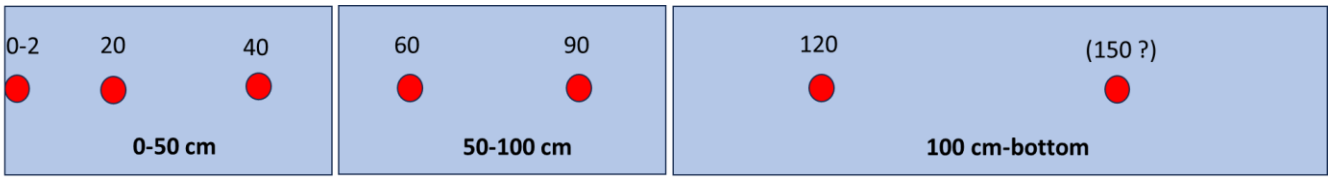

Figure 3. Schematic overview of the slicing of each long core collected from the experimental field area in the three sediment layers. The red dots correspond to the 7 layers where sediments for molecular analysis were collected.

2.3 Sampling campaigns for monitoring the ecosystem benefits and ecological sustainability of the applied in situ technologies

UNIVPM in joint collaboration with SZN elaborated a detailed sampling strategy for investigating the potential benefits for benthic biodiversity and ecosystems functioning of the in-situ remediation technologies based on a BACI (Before-After-Control-Impact) design. In particular, such design foresees the collection of replicated sediment samples in three different areas: i) an area in which the in situ remediation technologies in combination (TR1) or alone (TR2) will be tested, ii) an adjacent area in which the same operation for the installation of the in situ technologies will be done (i.e. artifact control) and iii) an other adjacent area to be used as control (Figure 4).

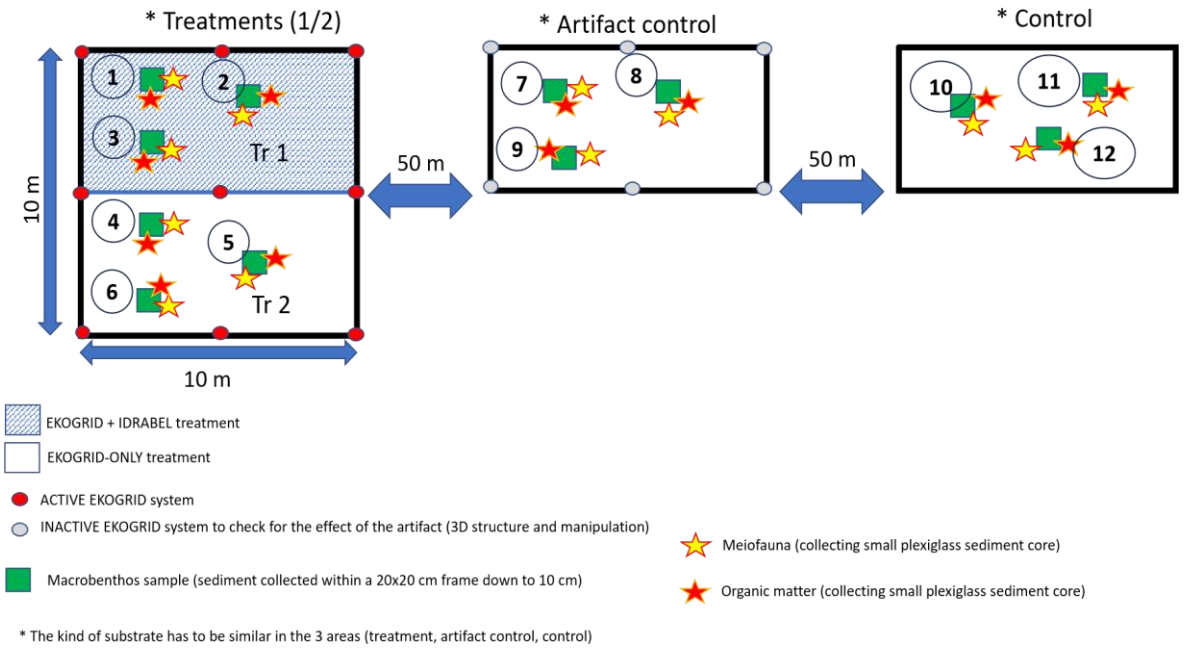

Figure 4. Schematic overview on the sampling design used for the monitoring of the potential ecosystem benefits and ecological sustainability of the selected remediation technologies.

Sediment samples (top 20 cm) have been collected in June, July and September 2023 by SZN professional SCUBA divers in all of these areas before *in-situ* remediation test and will be collected again during the remediation test (at least for the analysis of some variables) and after the end of the remediation trial. Monitoring activities on such samples include the analyses of the abundance, diversity and assemblage composition of meio- and macrofauna, the quantity and biochemical composition of organic matter (an index of the trophic state; Dell'Anno et al., 2022), and the determination of key attributes of ecosystem functioning in terms of extracellular enzymatic activities (i.e. as a proxy of organic matter degradation rates). For the determination of meiofaunal abundance and assemblage composition, organic matter biochemical composition and extracellular enzymatic activities, replicate plexiglass cores of sediments were randomly collected within the selected areas. For macrofauna, samples were collected within a 20x20 cm metal frame randomly positioned on the soft bottom within the selected areas using a bailer down to 10 cm within the sediment. The sediment was underwater transferred within labelled plastic bags and later on sieved on board of the research vessel using a 0.5 mm mesh. The sieved material was transferred into 2lt plastic jars and fixed using 70% alcohol.

For meiofaunal extraction, sediment samples were sieved through a 500-µm mesh, and a 20-µm mesh was used to retain the smallest organisms. The fraction remaining on the latter sieve was resuspended and centrifuged three times with Ludox HS40 (diluted with water to a final density

of 1.18 g cm^{-3}) according to Heip et al. (1985). All meiobenthic animals from 3 independent replicates per station were counted and sorted by taxa, under a stereomicroscope and after staining with Rose Bengal (0.5 g L^{-1}) (Bianchelli et al., 2010).

Macrofauna analyses were carried out at the Department of Biological and Environmental Sciences and Technologies – DiSTeBA of the Salento University. The identification was carried out to the lowest taxonomic level possible (mainly species) using stereo- and light microscope following proper identification manuals (see Appendix 1).

The quantity and biochemical composition of sediment organic matter were determined according to Fabiano and Danovaro (1998). Chlorophyll-a and phaeopigments were quantified using a spectrofluorometer after extraction with 90% acetone (24 h in the dark at 4°C) and their sum defined as total phytopigments (Danovaro and Fabiano, 1997). The main biochemical classes of organic compounds (proteins, carbohydrates, and lipids) were determined spectrophotometrically (Dell'Anno et al., 2002). The sum of carbohydrates, proteins, and lipids converted into C equivalents using the conversion factors 0.40, 0.49 and 0.75 mg C mg^{-1}, respectively was defined biopolymeric carbon (i.e. used as a proxy of trophic state, Dell'Anno et al., 2002).

Analyses of extracellular aminopeptidase (1-leucine-4-methylcoumarinyl-7-amide, Leu-MCA) and βD-glucosidase (MUF-b-glucopyranoside, Glu-MUF) activities were performed on sediment slurries prepared using 1:1 dilution (vol/vol) in 0.2 µm filtered and autoclaved seawater. Incubations were performed in the dark and at in situ temperature for 1 h. After evaluation of saturating conditions, enzymatic reactions were started by adding 200 µM of both Leu-MCA and Glu-MUF in three replicate sediment samples (Danovaro et al., 2001).

3. Results and interpretation

Due to the delay of the in-situ installation, monitoring results on remediation performance as well as on potential ecological effects are currently not available and are expected to be provided in the next deliverable related to Action B3 of the SEDREMED project (named "Final report with monitoring results"). Nevertheless, the chemical and ecotoxicological characterisation of the sediments collected in the pilot test site, the assessment of site-specific conditions, and particularly of natural attenuation processes of contaminants, and the assessment of the ecosystem health conditions in terms of biodiversity and key ecological attributes of the benthic site, are provided.

3.1 Monitoring the level and spatial variability of the chemical contamination in Bagnoli sediments

The concentrations of the different contaminants in the sediment samples collected in July 2022 were high (Table 1) and most of these exceed the available threshold values reported in the DM 173/2016 and D. Lgs. 172/2015 for sediment quality. Among the different contaminates analysed, PAH concentrations were highly variable among replicate samples (coefficient of variation = 75%), indicating a high heterogeneity of the distribution of these contaminants in the sediment even at small spatial scale, which need to be carefully taken into account for a robust assessment of the performance of the selected remediation technologies when applied in situ.

Table 1. Concentrations of the different contaminants analyzed in replicate sediment samples (R1, R2 and R3) collected in July 2022. Mean values and standard deviations (std) are also reported.

Compound	**Unit**	**R1**	**R2**	**R3**	**Mean**	**Std**
Al	mg/kg	20900	25900	25000	23933	2176
As	mg/kg	75	86	82	81.0	4.55
Cd	mg/kg	0.59	0.61	0.51	0.6	0.04
Cr	mg/kg	20.1	19.9	16.6	18.9	1.60

Cu	mg/kg	46.3	47.1	40	44.5	3.18
Fe	mg/kg	18400000	17000000	11800000	15733333	2839394
Hg	mg/kg	0.31616	0.33434	0.30909	0.32020	0.001
Ni	mg/kg	16	14.9	12	14.3	1.7
Pb	mg/kg	224	246	237	235.7	9.0
Zn	mg/kg	1080	1200	1080	1120	57
Hydrocarbons C>12	µg/kg	231000	339000	207000	259000	57411
Total PAHs	µg/	420000	109000	82000	203667	153

	k g					3 7

Based on the available ERM values for metals and PAHs (Long, 1995), the m-ERM- quotient values were calculated for both typologies of contaminants to classify sediments according to their potential ecotoxicological risk (Kowalska et al., 2018). The m-ERM-q values obtained from heavy metal concentrations allow classifying sediments at medium-high risk (Figure 5), while the m-ERMq values obtained from PAH concentrations allow classifying sediments from medium-low (replicate R2 and R3) to medium-high (replicate R1) risk.

Also in December 2022, the concentrations of several chemical contaminants analyzed greatly exceed the available threshold values reported in the D.M. 173/2016 and D. Lgs. 172/2015 for sediment quality (Table 2). At site L (low-contaminated) and also at site H (heavy-contaminated), the concentrations of most contaminants analyzed were similar or even higher in the 50-100 cm than in the 0-50 cm sediment layer. Such distribution of contaminants with depth in the sediment is consistent with that previously observed in the ABBACO project and further underlies the need to apply in situ remediation technologies able to efficiently reclaim not only the surface sediments but also the deeper sediment layers.

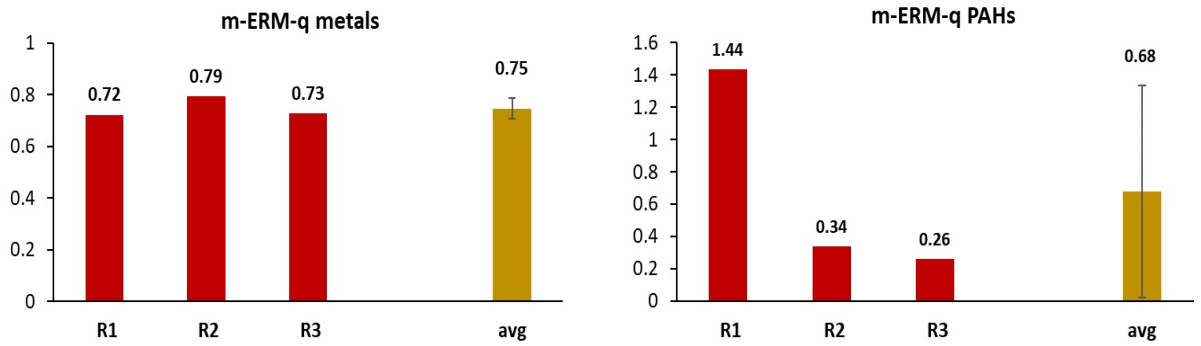

Figure 5. Values of m-ERM-q determined on the basis of heavy metal and PAH concentrations in replicated sediment samples collected in July 2022 with average values and standard deviation.

Table 2. Concentrations of chemical contaminants in the sediments (0-50 and 50-100 sediment layers) collected in December 2022 at the two sites (site L and site H) in the Bagnoli area.

		Sampling site				Sampling site			
		S i t e L	S i t e L	S i t e L	S i t e L	S i t e H	S i t e H	S i t e H	S i t e H

		Core A	Core A	Core B	Core B	Core A	Core A	Core B	Core B
Compound	Unit	0-50cm	50-1000cm	0-50cm	50-1000cm	0-50cm	50-1000cm	0-50cm	50-1000cm
Al	mg/kg	23800	23300	23700	24100	18000	15900	17100	19500
As	mg/kg	81	50	72	65	56	50	57	46
Ba	mg/kg	117	137	105	124	168	283	197	206
Cd	mg/kg	0.66	0.81	0.37	0.54	1.15	2.10	1.20	1.90
Cr	mg/kg	14.00	12.60	11.70	11.30	15.70	15.40	19.70	12.30
Fe	mg/kg	54000	50000	38500	40100	89000	93000	112000	78000
Mn	mg/	640	550	470	497	1350	1500	1560	1530

	kg								
Hg	mg/kg	0.27	0.36	0.21	0.27	0.42	0.75	0.42	0.59
Ni	mg/kg	7.20	6.20	5.50	5.10	10.20	8.90	13.00	7.10
Pb	mg/kg	200	231	166	198	283	417	295	378
Cu	mg/kg	64	74	61	61	46.0	50	50	42.3
Zn	mg/kg	560	496	422	463	890	1080	960	1110
Acenaphthene	µg/kg	8.0	52	18.4	21.8	91	174	115	174
Acenaphthylene	µg/kg	51	248	175	159	243	420	321	350
Anthracene	µg/kg	109	650	450	380	640	1170	730	1220
Benzo(a)anthracene	µg/kg	500	2570	1530	1510	1920	3700	2350	3000

Benzo(a)pyrene	µg/kg	870	43000	24100	23600	31000	66000	38000	50000
Benzo(b)fluoranthene	µg/kg	640	30000	18200	16500	24200	50000	28300	37000
Benzo(ghi)perylene	µg/kg	420	22400	12900	12300	16300	33000	19100	23800
Benzo(k)fluoranthene	µg/kg	320	16000	9300	9600	11900	23400	15200	18300
Chrysene	µg/kg	420	21700	13900	12900	16000	31000	19400	24000
Dibenzo(ah)anthracene	µg/kg	104	460	3000	280	360	660	440	500
Phenanthrene	µg/kg	173	10600	5200	5900	9200	19500	12100	20500
Fluoranthene	µg/kg	880	48000	29000	27300	40000	81000	48000	65000
Fluorene	µg/kg	17.20	99	57	67	127	3000	177	340
Indeno(123cd)pyrene	µg/	470	21	12	12	16	32	19	23

	kg		50	90	20	10	00	40	20
Naphthalene	µg/kg	31	64	70	67	133	310	450	450
Pyrene	µg/kg	800	3800	2450	2270	3400	9300	4100	5800
Total PAHs	µg/kg	5813	29263	176000	167885	233844	496244	286333	380144
Hydrocarbons C>12	mg/kg	51	63	34.60	47	67	145	71	93

Sediment samples of four layers (0-20 cm, 25-50 cm, 50-100 cm, >100 cm) collected in December 2022 were analyzed by ISO using additional monitoring tools based on GC-MS and SIM (single ion mode). These procedures allowed the quantification of specific PAH congeners and the determination of certain diagnostic ratios (Galperin et al, 2008). Sediment samples were treated by a Soxhlet procedure, and the extracts injected in a gas chromatograph (GC) coupled with a quadrupole mass spectrometer (qMS). The separation of hydrocarbons and identification of target compounds was achieved by a validated in-house procedure considering retention times, external standards and the NIST data base. Further hydrocarbon distribution patterns and diagnostic ratios were determined by single ion mode (SIM) chromatograms for substance- and compound-class specific mass fragments (e.g. methylated or alkylated compounds). Generally, the GC-MS patterns could not be attributed to a typical type of pollution (e.g. tar oil, heavy petroleum or diesel), which can be explained by long-term and very different contamination events. The concentration patterns of detected PAHs revealed major pollution occurring at different sediment depths of the investigated fields (Figure 6). Highest concentrations of PAHs (50 mg/kg) were found in the deep sediment layer (100 - ca. 130 cm) of pilot field H, while field L showed the highest value (20 mg/kg) at 25 - 100 cm depth. Remarkable small-scale heterogeneity was evident by comparing replicate sediment cores (A, B) collected at each site, where total PAHs varied up to twofold.

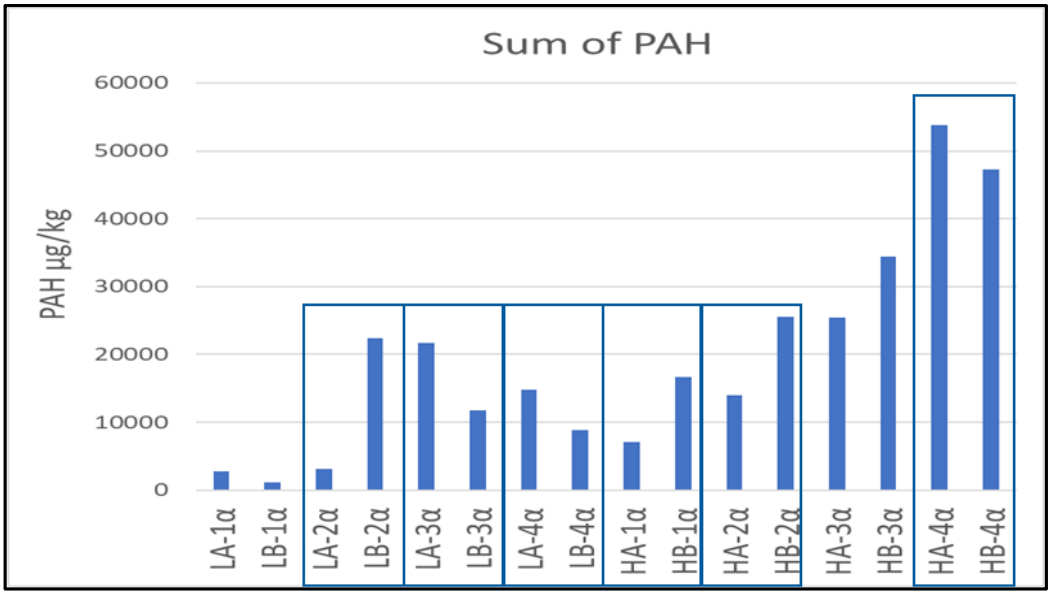

Figure 6. Amount of total PAHs determined by GC-MS analysis in sediment cores (A, B) of different layers (1: 0-20 cm; 2: 25-50 cm; 3: 50-100 cm; 4: >100 cm) from both pilot test sites (L, H). Replicate cores with remarkable heterogeneity (L-2/3/4α, H-1/2α) or elevated PAH concentrations (H-4α) are highlighted by frames.

Regarding specific compounds, PAHs were generally dominated by fluoranthene and pyrene, but in some cases high concentrations of phenanthrene, dibenzofurane and dibenzothiophene were also observed (Figure 7). In contrast to the varying PAH level, the spectrum of PAH compounds was rather similar at both sites. SIM analyses revealed a lower load of methylated PAHs, since only methylated pyrenes and chrysenes were identified. The profiles of PAH pollution were rather similar in the investigated locations though, occasionally, singular compounds showed exceptional heights (e.g. phenanthrene and dibenzothiophene in HB-3·).

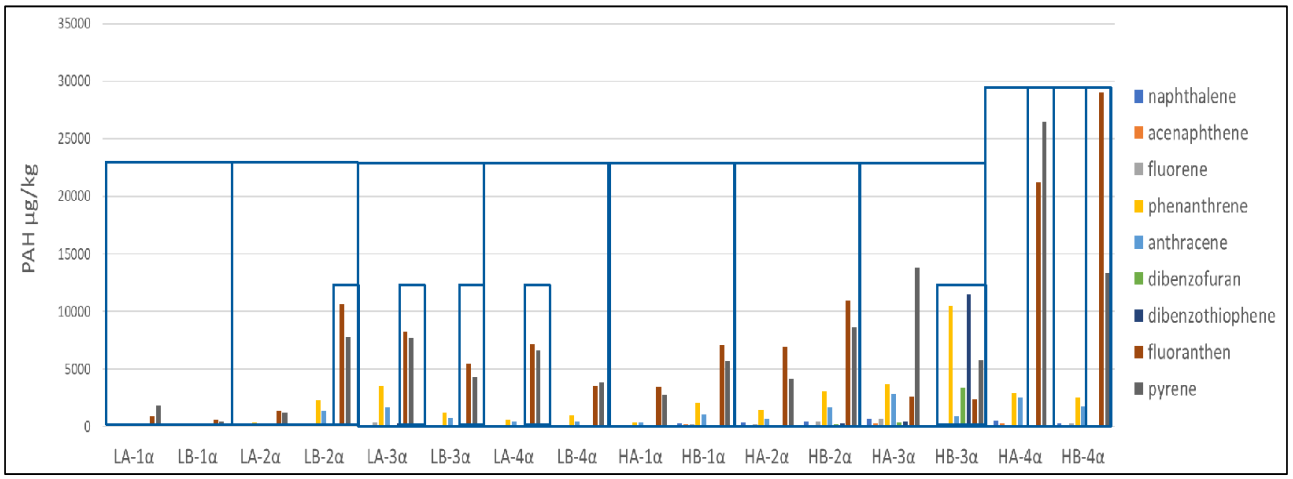

Figure 7. Amount of specific PAHs in the sediment cores (A, B) of different layers (1: 0-20 cm; 2: 2550 cm; 3: 50-100 cm; 4: >100 cm) from both pilot test sites (L, H). Dominating compounds are highlighted by small frames.

3.2 Monitoring the background of chemical contamination and ecotoxicological risk of Bagnoli sediments in the experimental field sites

Here we show the results on chemical contamination and ecotoxicological risk of Bagnoli sediments in the experimental field area, analyzed from sediment samples collected in November 2023, during the *in-situ* installation of selected technologies.

3.2.1 Chemical contaminant concentrations in experimental field area

Results of chemical analysis revealed PAH concentrations approximately 50 times higher in the deepest sediment layer (100 cm-bottom) than those in the 0-50 cm sediment layers (Figure 8).

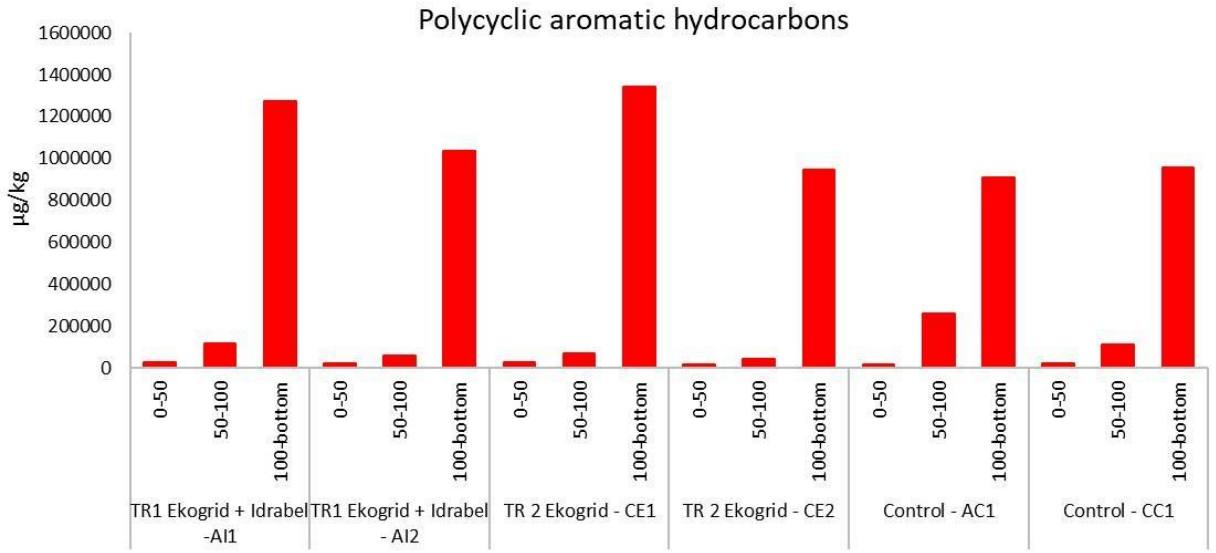

Figure 8. Concentrations of PAHs expressed in µg/kg in the three layers of the six cores collected from experimental field area. TR1: treatment area with both EKOGRID and IDRABEL technologies; TR2: treatment with only EKOGRID technology.

Similar trend has been observed considering also the heavy hydrocarbons (C≥12) and the PCB, which displayed concentrations approximately 15-20 and 10 times higher in the deepest layer (100 cm, bottom) than those in the 0-50 cm and 50-100 cm sediment layers, respectively (Figure 9 and Figure 10).

Also, heavy metals displayed an increase of concentrations from the surface down to the deeper sediment layers, with the only exception of NI and As (Figure 11). In particular, Ni concentrations were characterized by similar values among all the layers considered, whereas As concentrations displayed the highest values in the top 0-50 cm sediment layer.
In all sediment samples Cr and Ni concentrations were below the threshold contamination values established by the Italian decree 172/2015 for marine sediments, whereas Pb, Ni and As concentrations exceeded such values (Figure 11).

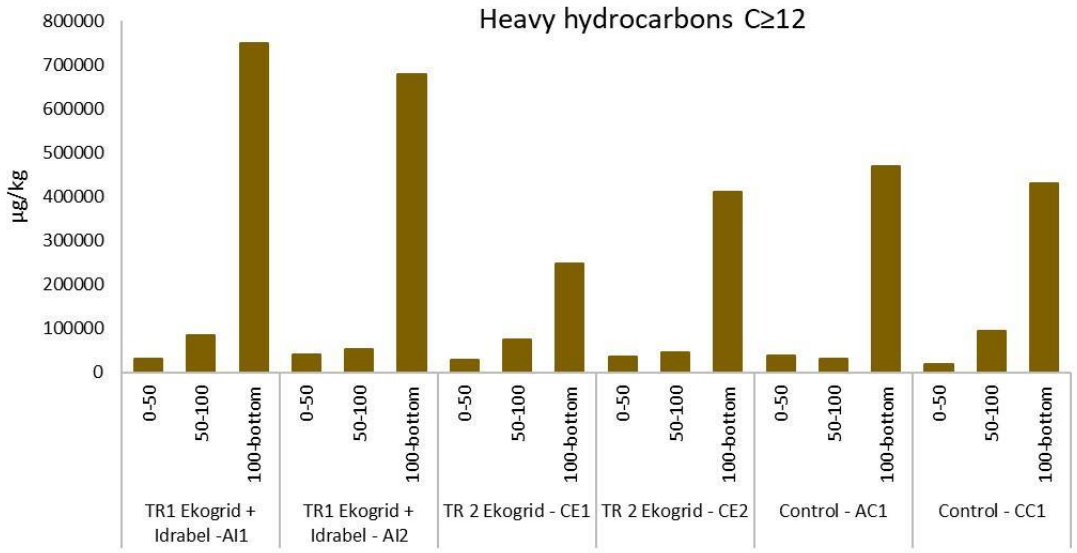

Figure 9 . Concentrations of heavy hydrocarbons (C≥12) expressed in µg/kg in the three layers of the six cores collected from experimental field area. TR1: treatment area with both EKOGRID and IDRABEL technologies; TR2: treatment with only EKOGRID technology.

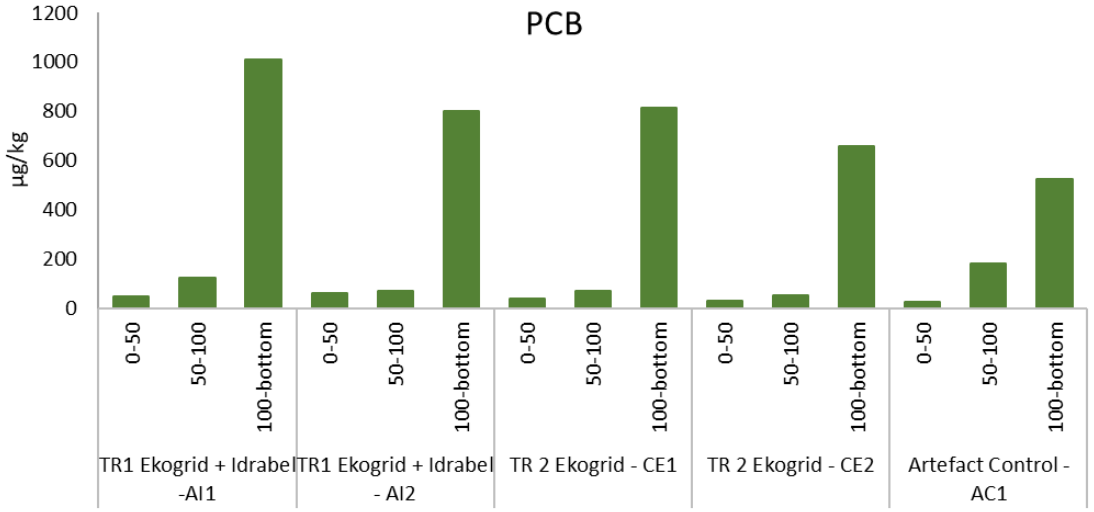

Figure 10. Concentrations of PCB expressed in µg/kg in the three layers of the six cores collected from experimental field area. TR1: treatment area with both EKOGRID and IDRABEL technologies; TR2: treatment with only EKOGRID technology.

Figure 11. Concentrations of heavy metals expressed in mg/kg in the three layers of the six cores collected from the experimental field area. TR1: treatment area with both EKOGRID and IDRABEL technologies; TR2: treatment with only EKOGRID technology. The concentrations in red are the threshold values for those heavy metals, according to the Italian decree 172/2015 (i.e. Environmental Quality Standard).

3.2.2 Ecotoxicological bioassays and level of hazard (WOE-LOE)

The results of the biological assay carried out with *A. fischeri* indicate a substantial absence of toxicity for all samples, with the exception for the bottom layer of samples AI1, AI2, AC1 and CC1 (Figure 12). The results from the algal growth inhibition bioassay with the algae *P. tricornutum* highlighted a phenomenon of biostimulation of algal growth, however 3 samples showed a percentage of inhibition of algal growth between 3% (CE1 050-100 cm) and 49 % (AI2 050-100 cm) (Figure 12). The results of the embryotoxicity bioassay carried out on *C. gigas* showed a percentage abnormal larva above 50% in all samples, only one sample showed a lower percentage of approximately 30% (Figure 12).

Results of the bioassays has been elaborated through a quantitative weight of evidence model (sediqualsoft developed by UNIVPM and the Italian Institute for Protection and Environmental Research - ISPRA), which assigns to each bioassay specific thresholds and weights based on the measured endpoint and sensitivity of the tested species, to finally provide a cumulative level of hazard of the entire bioassays battery. Based on these criteria, each sample of sediment are assigned to one of five classes of hazard, which are Absent, Slight, Moderate, Major and Severe (Table 12).

The deepest sediment layers displayed a higher level of ecotoxicological hazard than surface sediments (Moderate to Major).

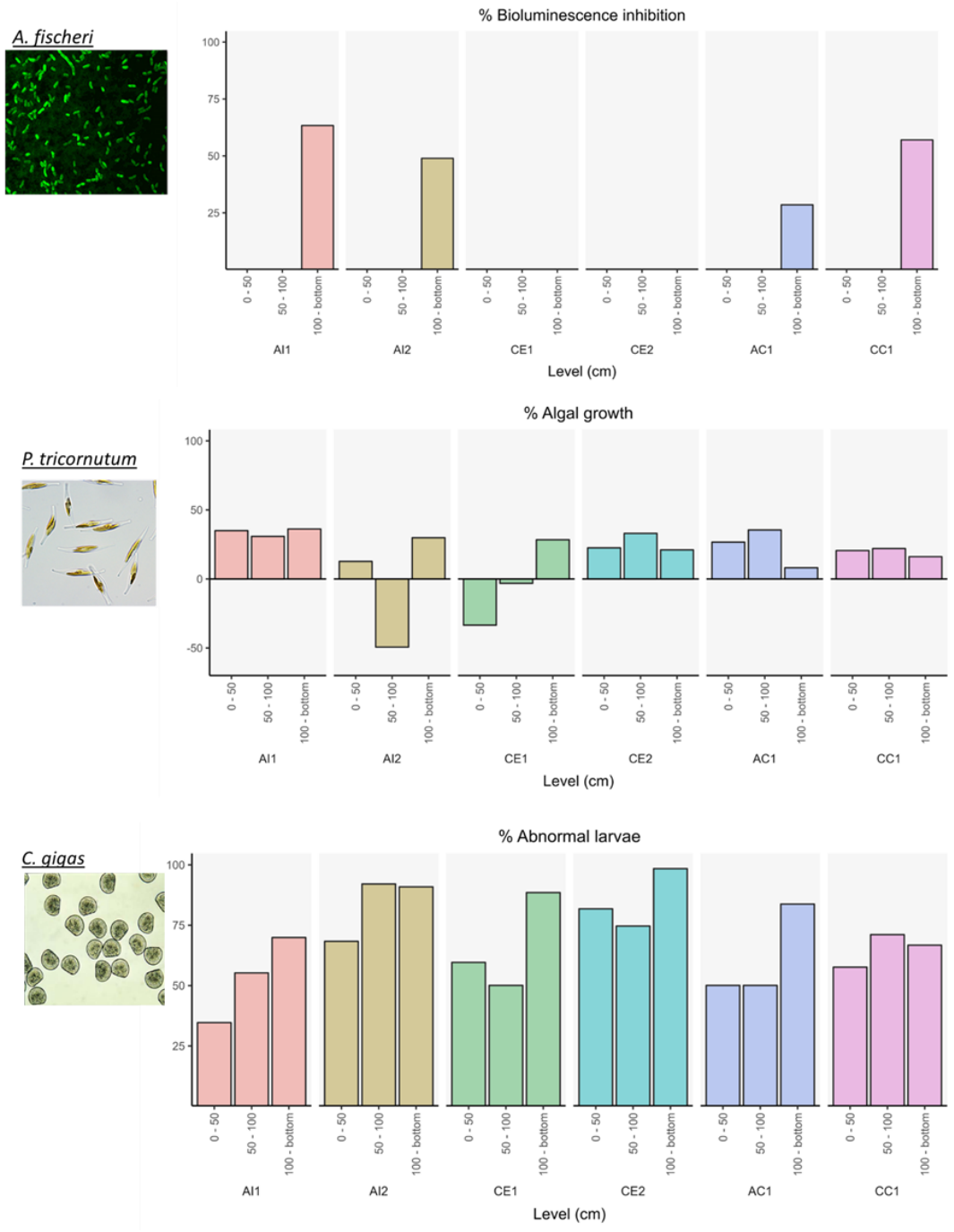

Figure 12. Ecotoxicological assay according to Italian DM 173/2016, using 3 different biological assays: bioluminescence inhibition (%) of Aliivibrio fischeri, growth inhibition (%) of Phaeodactylum tricornutum, embryotoxicity (% of abnormal larvae) of Crassostrea gigas.

Table 3. Cumulative level of ecotoxicological hazard for each sediment samples, calculated on bioassay specific thresholds and weights based on the measured endpoint and sensitivity of the tested species.

Sample	Level	$HQ_{Battery}$	Level of hazard ecotoxicological
TR1	0-50 cm	0.7	ABSENT
	50-100 cm	0.7	ABSENT
	100-bottom	2.5	MODERATE
AI1	0-50 cm	0.5	ABSENT
	50-100 cm	0.8	ABSENT
	100-bottom	3.5	MAJOR
AI2	0-50 cm	1.0	ABSENT
	50-100 cm	2.6	MODERATE
	100-bottom	3.5	MAJOR
CC1	0-50 cm	0.8	ABSENT
	50-100 cm	1.0	SLIGHT
	100-bottom	3.2	MAJOR
CE1	0-50 cm	1.2	SLIGHT
	50-100 cm	0.7	ABSENT
	100-bottom	1.5	SLIGHT
CE2	0-50 cm	1.3	SLIGHT
	50-100 cm	1.1	SLIGHT
	100-bottom	1.7	MODERATE

3.3 Monitoring tools for in situ assessment of the natural attenuation capacity in Bagnoli sediments

To provide insights on the natural attenuation capacity of the autochthonous microbial assemblages toward hydrocarbons (i.e., the capacity of the microbial assemblages to degrade hydrocarbons without any biostimulation/bioaugmentation treatments) several innovative monitoring tools have been applied.

3.3.1 *Diagnostic Ratios of Specific Polyaromatic Compounds*

Ratios of specific polyaromatic compounds can provide insights on particular contamination processes or periods, the degree of degradation and weathering (Galperin et al, 2008). PAH with easier degradable bonds is more rapidly eliminated than more stable ones so that their ratio will change due to microbial decomposition. Thus, several diagnostic ratios are available for the

assessment of PAH degradation. Considering diagnostic ratios at the investigated fields (Table 4), alkylated PAHs (e.g. methylpyrene) did not display a relevant increase compared to the nonsubstituted PAHs (e.g. pyrene), so that only limited PAH degradation could be concluded. However, the peaks of alkylated PAHs were often disturbed by high amounts of non-substituted PAHs so that the respective rations were difficult to evaluate. Nevertheless, ratios of phenanthrene/anthracene as well as methylpyrene/pyrene could be determined for most of the samples. However, the rations were fairly similar and didn't indicate degradation processes. The value in HB-3· can be treated as an outlier, since also the pollution profile is exceptional. At least, the determined diagnostic ratios provide a valuable baseline for the evaluation of technological treatments, where they might alter due to contaminant degradation.

Table 4. Diagnostic ratios (peak heights) of specific polyaromatic compounds, indicating degradation by their increase (↑). nd = at least one compound was not detectable.

Pollution Level Field	Low	Low	Low	Low	Low	Low	Low	Low	High	High	High	High	High	High	High	High
Depth	0-25	0-25	25-50	25-50	50-100	50-100	>100	>100	0-25	0-25	25-50	25-50	50-100	50-100	>100	>100
Core	A	B	A	B	A	B	A	B	A	B	A	B	A	B	A	B
Sample Identifier	LA-1α	LB-1α	LA-2α	LB-2α	LA-3α	LB-3α	LA-4α	LB-4α	HA-1α	HB-1α	HA-2α	HB-2α	HA-3α	HB-3α	HA-4α	HB-4α
Acenaphthene/Fluorene ↑	nd	nd	nd	nd	nd	nd	nd	nd	0,9	0,8	0,5	nd	0,4	nd	nd	nd
Dibenzofurane/Fluorene ↑	nd	nd	nd	nd	0,7	nd	nd	nd	0,2	0,7	nd	0,6	0,7	nd	nd	nd
(C2-Napht+C3-Naphth)/Napht ↑	nd	nd	nd	nd	nd	nd	nd	nd	nd	nd	nd	nd	nd	nd	nd	nd
Phenanthrene/Anthracene ↑	nd	nd	1,7	1,7	2,1	1,7	1,3	2,1	1,1	2,0	2,1	1,9	1,3	11,3	1,1	1,4
(C2-Dibenzothioph+ C3-Dibenzothioph)/(Dibenzothioph) ↑	nd	nd	nd	nd	nd	nd	nd	nd	nd	nd	nd	nd	nd	nd	nd	nd
((C2-Anthr+Phen+(C3-Anthr+Phen))/(Anthr+Phen) ↑	nd	nd	nd	nd	nd	nd	nd	nd	nd	nd	nd	nd	nd	nd	nd	nd
Methylpyrene/Pyrene ↑	nd	nd	0,4	nd	nd	nd	0,1	nd	0,1	nd	0,3	0,4	0,3	1,0	0,2	nd

3.3.2 Metabolite Analysis

Metabolite analysis represents a simple and quick method for providing evidence of *in-situ* biodegradation (Morasch et al., 2011) and its potential enhancement due to the application of the selected SEDREMED technologies. It is applicable to a wide variety of aromatic and aliphatic hydrocarbons and allows discriminating between aerobic and anaerobic degradation processes. Metabolites were analyzed in diluted pore water of sediments from different layers (500 mL clean distilled water in 100 g sediment), which have been collected in December 2022 in the Bagnoli test site. The metabolite extraction, derivatization and subsequent analysis using GC-MS were carried out using an adapted in-house (ISO) procedure. The metabolites were identified by comparing mass spectra and retention times with those of laboratory metabolite standards. In all analyzed sediment samples, no specific metabolites of the aerobic/anaerobic PAH degradation were detected. However, the detection of benzoates revealed miscellaneous natural degradation of PAH at the Bagnoli test site (Table 5).

Table 5. Metabolites from potential aerobic/anaerobic PAH degradation pathways in sediment samples of different layers at test sites (L and H); nd= below detection limits.

sample ID	HA-1a	HA-2a	HA-3a	HA-4a	LA-4a	LB-1a
unit	µg/kg	µg/kg	µg/kg	µg/kg	µg/kg	µg/kg
Metabolites of aerobic BTEX biodegradation						
Catechol (1,2-dihydroxybenzene)	nd	nd	nd	nd	nd	nd
Methylcatechol (Dihydroxytoluene)	nd	nd	nd	nd	nd	nd
Ethylcatechol	nd	nd	nd	nd	nd	nd
Benzyl alcohol	nd	nd	nd	nd	nd	nd
Metabolites of aerobic Naphthalene biodegradation						
1-Naphthol (1-Hydroxynaphthalene)	nd	nd	nd	nd	nd	nd
2-Naphthol (2-Hydroxynaphthalene)	nd	nd	nd	nd	nd	nd
1,2 or 2,3-Dihydroxynaphthalene	nd	nd	nd	nd	nd	nd
Metabolites of anaerobic BTEX biodegradation						
Benzylsuccinic acid	nd	nd	nd	nd	nd	nd
(1-phenylethyl)benzylsuccinic acid	nd	nd	nd	nd	nd	nd
(2 and/or 3 and/or 4)-Methylbenzylsuccinic acid	nd	nd	nd	nd	nd	nd
Metabolites of anaerobic Naphthalene biodegradation						
(1 and/or 2)-Naphthoic acid	nd	nd	nd	nd	nd	nd
5,6,7,8-tetrahydro-2-Naphthoic Acid	nd	nd	nd	nd	nd	nd
Metabolites of anaerobic PAH biodegradation						
Naphthylmethylsuccinic acid	nd	nd	nd	nd	nd	nd
Phenanthrene-4-carboxylic acid or 9-Anthracencaboxylic ac	nd	nd	nd	nd	nd	nd
Flouren-9-carboxylic carboxylic acid	nd	nd	nd	nd	nd	nd
Acenaphthene- 5 and/or 3 -carboxylic acid	nd	nd	nd	nd	nd	nd
Metabolites of aerobic and anaerobic mono- and polycyclic aromatic hydrocarbon biodegradatio						
Benzoic acid	+/-	10	32	24	25	62
(2 and/or 3 and/or 4)-Hydroxybenzoic acid	nd	nd	nd	nd	nd	nd
2,5-Dihydroxybenzoic acid (Gentisic acid)	nd	nd	nd	nd	nd	nd
3,4-Dihydroxybenzoic acid (Protocatechuic acid)	nd	nd	nd	nd	nd	nd
o/m/p-Toluic acid (methylbenzoic acid)	nd	nd	nd	nd	nd	nd
Phenol (probably co-contamination)	nd	nd	nd	nd	nd	nd
o/m/p-Cresol (probably co-contamination)	nd	nd	nd	nd	nd	nd
Metabolites of anaerobic alkane biodegradation						
Alkylsuccinic acids	nd	nd	nd		nd	nd

n.d. = not detected, below limit of detection

+ = detected, but quantification not possible due to peak overlay

+/- = detected, but below limit of quantification

3.3.3 Compound-specific isotope analysis

To prove and quantify biodegradation, component-specific isotope analysis of carbon (13C/12C CSIA) has become a key method for different chemical contaminants (e.g., BTEX, PAH; US EPA 2008). It is based on the concentration decrease and concomitant enrichment of the heavy C

isotope (^{13}C) due to biodegradation. CSIA can be used not only to elucidate pollutant degradation, but also to discriminate contaminant sources by their isotopic fingerprint. However, it is generally limited to small molecules with less than 12 carbon atoms. Concentration analysis and selective CSIA carried out on sediment samples collected in December 2022 in Bagnoli test sites indicated that, except naphthalene, all detected pollutants had more than 12 carbon atoms so that CSIA was not feasible to provide evidence for biodegradation.

3.3.4 BACTRAPS

BACTRAPS are *in-situ* microcosms containing substrates amended with an adsorbed 13C-labeled contaminant. During their exposition in sediments, the substrates can be colonized by pollutantdegrading microorganisms, which assimilate the 13C-label into their biomolecules such as amino acids (AA) and fatty acids (Bahr et al, 2015). The analysis of 13C accumulation in these biomolecules will provide a semi-quantitative comparison of local biodegradation performance. ISO developed special lancets containing microcosms with isotope-labelled polycyclic aromatic hydrocarbons (BACTRAPS). They were inserted on November 4th, 2022, at two different depths into the sediment (0-15 cm and 20-35 cm) of each test field, and successfully recovered on January 27th 2023, after 83 days of in situ exposition.

Amino acid concentration analysis from extracted BACTRAP biofilms revealed microbial colonization (1,7 - 2,5 mg total AA per BACTRAP) in 6 from 8 BACTRAPS (Figure 13). However, the respective ^{13}C AA isotope values ranged between -2 ‰ and +10 ‰. Generally, ^{13}C values of amino acids are negative and vary between -74 ‰ and 0 ‰. Occasionally, they can reach values up to +11 ‰ depending on the utilized substrate. As the detected AA isotope values are significantly above 0 ‰, minor assimilation of the isotope label into microbial biomass can be assumed. Thus, a weak indication of *in situ* PAH degradation was observed. In contrast, the failing performance of two BACTRAPS both placed in the heavy-contaminated field at 30 cm depth, is a hint for potential toxic conditions at certain sediment spots. Here, the extraction of amino acids was exceptionally inhibited by an unknown chemical substance. Moreover, also the deuterium-labeled BACTRAPS didn't show a significant isotope enrichment of amino acids. However, this unproven BACTRAP approach with deuterated compounds has been primarily tested so that these results are not valid for distinct conclusions.

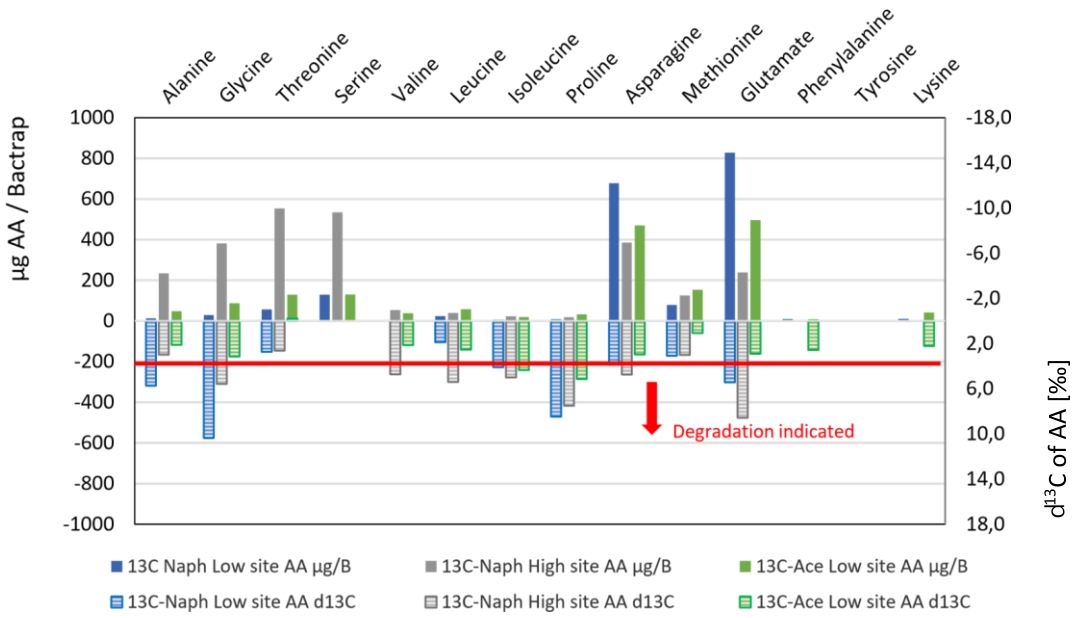

Figure 13. Columns upwards: Amount of microbial colonization (denoted as amino acid concentration AA) in BACTRAPS (loaded either with ^{13}C-naphthalene or ^{13}C-acenaphthene) from sediment layers at both field sites (H: 30 cm Naph; L: 15 cm Naph, 30 cm Ace). Columns downwards: Isotope values of respective amino acids, occasionally showing weak indication (>2 ‰) of contaminant degradation.

3.3.5 Molecular analyses for the monitoring of the microbial degraders

Molecular analyses of microbial communities can provide additional information on the treatment effects due to the selected technologies. This can be achieved either by community analysis based on next generation sequencing (NGS) or by qPCR analysis targeting specific microbial taxa and genes (Table 6). Different primers are currently considered for application in a number of SEDREMED samples from field, micro- and mesocosms. For cost-saving reasons, they will be analyzed by SZN in an extended analytical run in the current year together with samples from treated sediments.

Table 6. Molecular tools to analyze microbial assemblages in the field and in mesocosm/microcosm samples.

Bulk Community Analysis
Next Generation Sequencing NGS
Taxonomic Composition of the Microbial Community

Specifying Population Analysis
Functional Marker Genes qPCR
16SrDNA (total eukaryotes)
Benzylsuccinate synthase (toluene degradation)
Ethylbenzene dehydrogenase
Benzyl-CoA reductase (BTEX-degradation)
Oxoacyl-CoA hydrolase (anerobic BTEX-degradation) central metabolism BTEX
Naphthoyl-CoA reductase (anaerobic Naphthalene degradation) Naphthalene specific
Catechol 2,3-dioxygenase (aerobic BTEX/PAH degradation) central metabolism BTEX/PAH
Aliphatic Hydrocarbons?

3.4 Monitoring ex situ bioremediation performance of the selected technologies

3.4.1 Laboratory microcosms

• Degradation of PAH compounds

Ad hoc microcosms experiments using Bagnoli sediments were carried out by UNIVPM and SZN to test the performance of IDRABEL Bio-Vase product on the degradation of PAHs. Bio-Vase product developed by IDRABEL basically contains selected microbial strains fixed to a mineral porous media and it is thought to increase biodegradation performance of organic pollutants once added to the sediment. Moreover, the zeolite carrier material can be assumed to adsorb heavy metals as well as other pollutants.

In a first set of laboratory experiments, PAH concentrations of sediments of Bagnoli collected in July 2022 were monitored over time to estimate the biodegradation performance of the IDRABEL product in comparison with other treatments (Dell'Anno et al., 2020). Three different aerobic treatments with IDRABEL Bio-Vase product and a fourth one without any amendment (control, CTRL) have been used during time-course incubations lasting ca. 2 months. Treatment 1 was based on the addition of sterilized Bio-Vase product, treatment 2 was based on the addition of the original Bio-Vase product (i.e., containing fixed microorganisms), treatment 3 was based on the addition of specific bacterial and fungal strains (previously isolated from contaminated Bagnoli sediments) to sterilized Bio-Vase product. The Bio-Vase product to sediment ratio was 1:60 w/w.

All microcosms (n=12) were incubated in aerobic conditions using natural seawater at 20°C. In all microcosms, the concentrations of sixteen PAH congeners have been analyzed by collecting sediment sub-samples immediately after the beginning of the experiment and after ca. 1 month and 2 months of incubation.

Sediments used for assessing the bioremediation performance on PAHs were characterized by different initial concentrations, especially in terms of low molecular weight congeners (Figure 14). Such variability of concentrations was even evident between replicate samples of the same treatment. Overall, total PAH concentrations at the end of time-course experiments decreased in treatment 1 (sterilised Bio-Vase), treatment 2 (Bio-Vase with fixed microorganisms) and in the control (without amendments; Figure 14). Generally, a decrease of low molecular weight PAHs was observed. Treatment 3 did not determine a remarkable decrease of PAHs over time.

On the basis of these results, it has been estimated that the allochthonous microbial assemblages present in the Bagnoli sediment can degrade after ca. 2 months of incubation ca. 60% of total PAH concentrations under aerobic conditions, suggesting a high natural attenuation capacity toward these contaminants when molecular oxygen is available. However, anaerobic conditions prevail in Bagnoli sediments (below 15-20 cm depth), but it has to be regarded that the EKOGRID technology could provide a remarkable switch of redox conditions close to aerobic level. The addition of BioVase slightly improved the degradation yield, especially for the low molecular weight PAH congeners. Moreover, Bio-Vase might have a positive effect on the adsorption/immobilisation of heavy metals, which still needs to be assessed. The degradation yields assessed by such experiments should be viewed with caution due to the high variability of PAH concentrations between replicated assays and somehow artificial laboratory conditions.

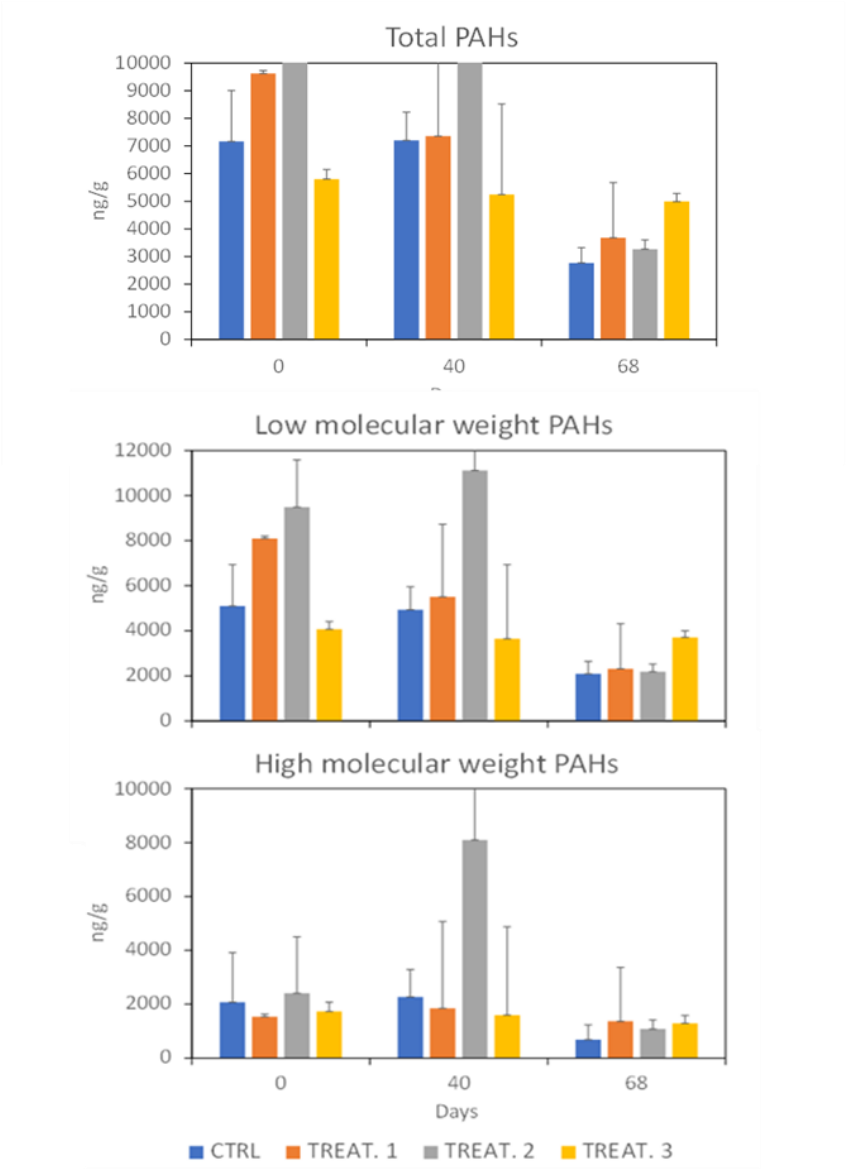

Figure 14. Concentrations of total, low and high molecular weight PAH congeners in the treated sediments and in the control (CTRL) during the time-course experiments.

• Mineralization of Isotope-Labeled PAH compounds

A second set of microcosm experiments for assessing the performance of the IDRABEL Bio-Vase product has been carried out by ISO using different sediment layers collected in Bagnoli in December 2022. In such laboratory experiments the mineralization rates (i.e., degradation down to end-products) of spiked 13C-labeled hydrocarbons (Bahr et al., 2015) to the sediments were monitored over time. Mineralization of the spiked 13C-labeled hydrocarbons showing up in end products (i.e. 13C-CO_2) can be proven for defined environmental conditions and even quantified by mass balance calculations.

A total of 67 laboratory microcosms were set up either with 13C-labeled naphthalene or phenanthrene. Mineralization was compared between sediments from different depths (0-25 cm, 25-50 cm, 50-100 cm, >100 cm) and from both the test sites (sites L and H). Furthermore, the assays were carried out using different amounts of Bio-Vase product (1:60; 1:5) provided by IDRABEL, mimicking either anaerobic or aerobic conditions, which occur along the sediment profile of the Bagnoli sites. To check potential abiotic reactions, inactivated controls were prepared.

Aerobic microcosms from both sites without Bio-Vase product displayed an immediate and intense mineralization of phenanthrene and naphthalene, independently from sediment depth (blue curves, Figures 15 and 16). In contrast, microcosms amended with Bio-Vase (1:60) plus oxygen support revealed a long lag-phase (> 50 days) followed by low mineralization rates of PAH (yellow curves). Notably, high oxygen consumption in comparison to microcosm assays without Bio-Vase was observed. Thus, the Bio-Vase product initially stimulated aerobic microorganisms, yet not those performing PAH degradation. Moreover, anaerobic PAH mineralization was proven by these microcosm experiments, though with occasionally long lag-phases (green curves). For phenanthrene, it started after approximately 70 days of incubation in the surface sediment layer. Anaerobic mineralization of naphthalene started much faster (occasionally <5 days after incubation) and was evident with sediments collected at depth down to 100 cm. Therefore, we conclude that natural attenuation of *dissolved* PAH is evident in Bagnoli, yet highly diverse for specific PAHs.

Generally, the behavior of microcosms from different cores (within the same sites) was very similar. Thus, a widespread potential for fast aerobic and slower anaerobic microbial PAH degradation can be assumed despite local heterogeneity of contaminant distribution. Probably, the EKOGRID technology will cause a discharge of electrons and thus create virtually aerobic conditions. This would definitely stimulate the elimination of dissolved contaminants. Further tests have to clarify the behavior of sorbed pollutants.

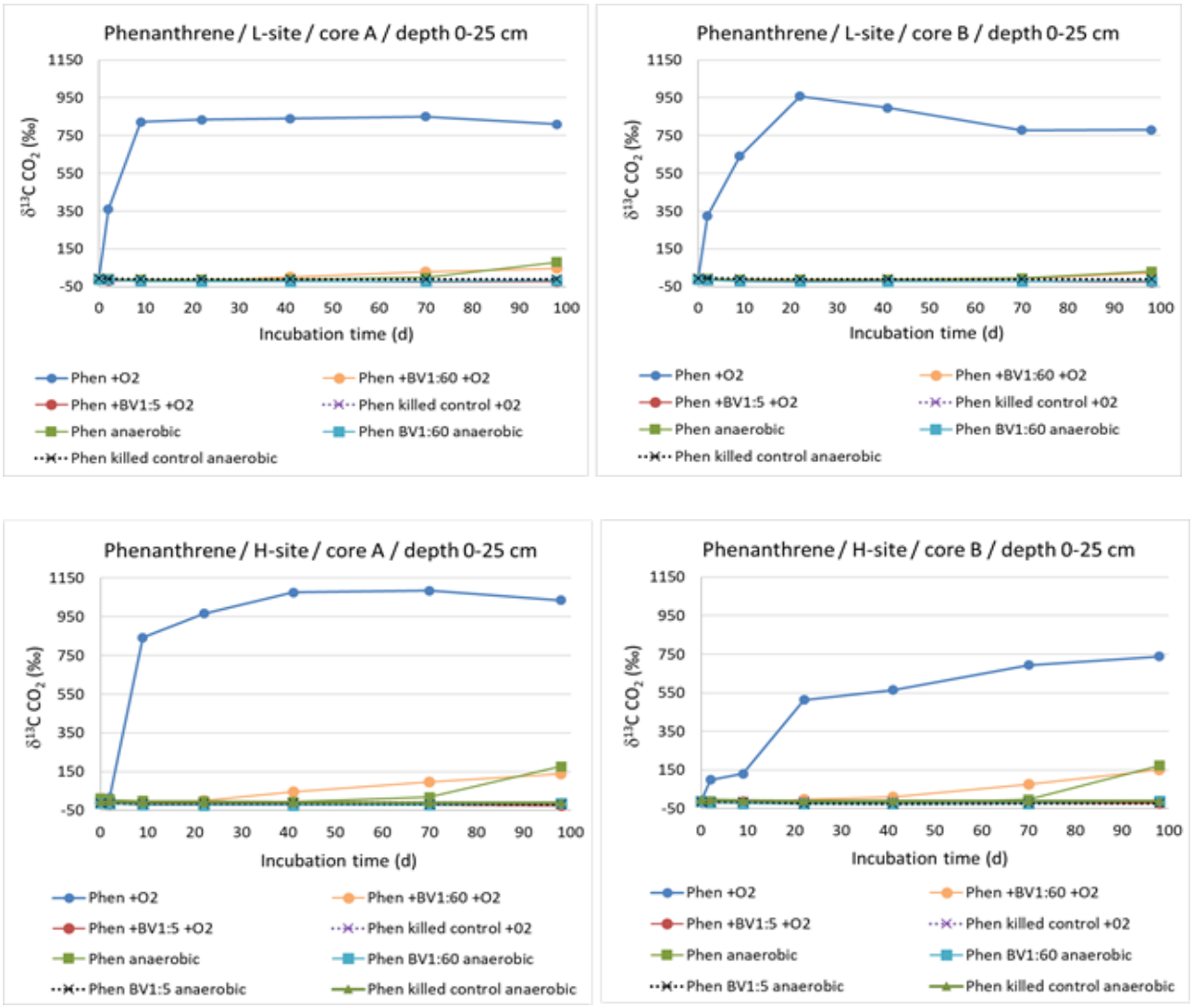

Figure 15. Mineralization (shown as ^{13}C isotope value from end product CO_2) of spiked ^{13}Cphenanthrene to Bagnoli sediments (0-25 cm sediment layer) collected at both test sites (L, H) and containing various amounts of IDRABEL Bio-Vase product during assays carried out in anaerobic or aerobic (by continuous O_2 supply) conditions.

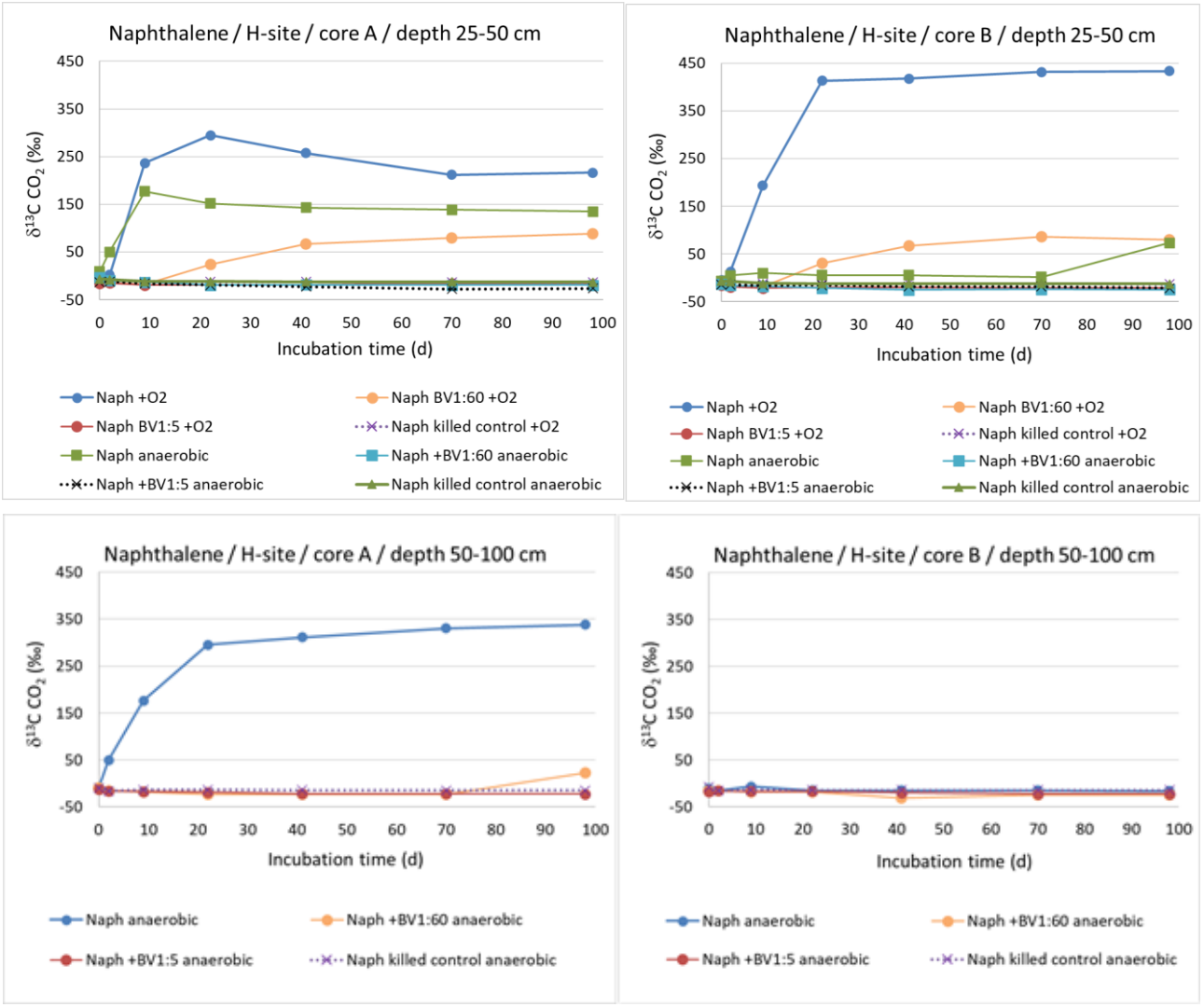

Figure 16. Mineralization (shown as ^{13}C isotope value from end product CO_2) of spiked ^{13}C-naphthalene to Bagnoli sediments of different layers (25-50 cm and 50-100 cm) collected at both test sites (L, H) and containing various amounts of IDRABEL Bio-Vase product during assays carried out in anaerobic or aerobic (by continuous O_2 supply) conditions.

• Assessing the potential release and adsorption of metals by the IDRABEL products

Further microcosm experiments were carried out by UNIVPM and SZN to test the potential release and adsorption of the heavy metals by the IDRABEL Bio-Vase. Three different typologies of IDRABEL Bio-Vase products were tested: (1) BIO-VASE PRE-BIOFIXED product, that represents the microporous inorganic substrates (i.e. the microporous inorganic support matrix without biofixed microorganisms); (2) BIO-VASE AEROBIC product, the commercial product designed for applications in an oxygenated environment (i.e. made up of microporous inorganic substrates with a formulation of biofixed aerobic microorganisms); (3) BIO-VASE ANAEROBIC product, the commercial product designed for applications in hypoxic/anoxic environment (i.e. the microporous inorganic substrates and a formulation of biofixed anaerobic microorganisms).

Bio-Vase products were added in 6 sterile tubes with sterile artificial sea water (1 g of Bio-Vase product in 3 ml of artificial sea water). Each Bio-Vase product type was added in two tubes: one used to monitor the eventual release of heavy metals by the product itself; one in which six heavy metals were added (Mn, Zn, Fe, Cu, Pb, Ni; each at a concentration of 100ppm) to test the heavy metals' adsorption efficiency of the IDRABEL products.

Microcosms containing the PRE-BIOFIX and AEROBIC products were incubated in aerobic conditions, while microcosms containing the ANAEROBIC product were incubated mimicking anaerobic conditions. In all microcosms, the concentrations of heavy metals were analyzed with ICP-OES in subsamples collected after 7 days (Time 1) and 12 days (Time 2) from the beginning of the experiment.

Moreover, each product (as dry powder) was also analyzed to evaluate the concentration of heavy metals contained in the product itself.

The results showed that all Bio-Vase products contain variable concentrations of heavy metals. The concentrations of Pb and Cd exceed the acceptability levels (L1 limit of Italian decree 173/2016) in all Bio-Vase products, and the concentrations of Zn and As exceed the threshold levels (L1 limit) of the Italian decree 173/2016 in AEROBIC and ANAEROBIC products, respectively (Figure 17).

Despite the evidenced contents of heavy metals within the products, the release tests indicated that all Bio-Vase products, at the conditions tested in the laboratory, did not release relevant amounts of heavy metals in seawater (Figure 17).

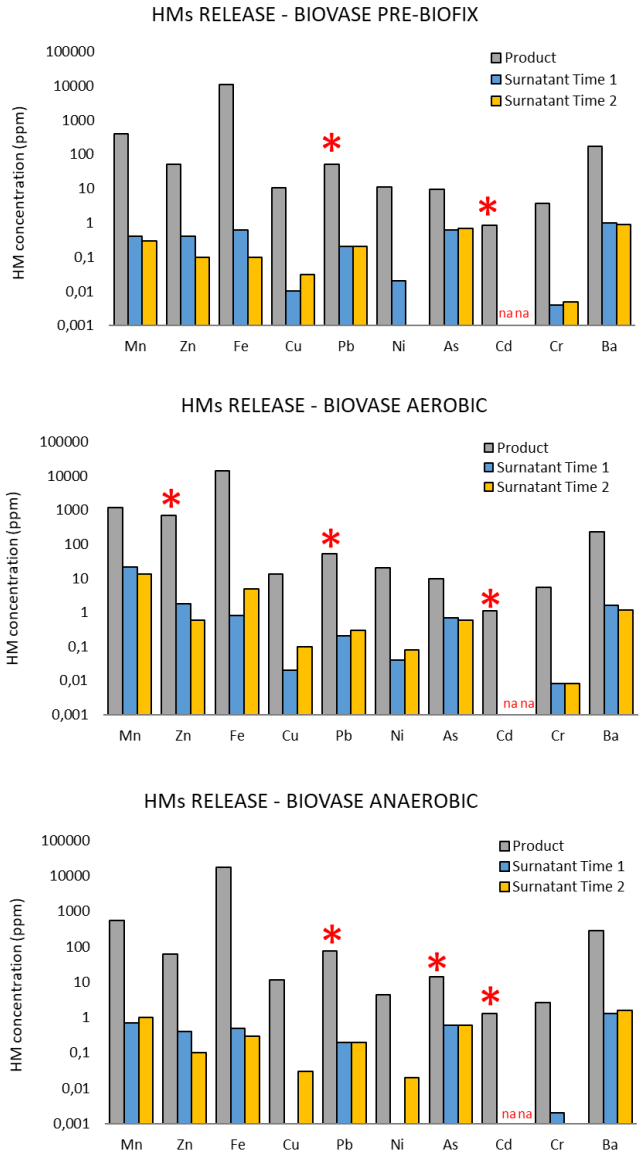

Figure 17. Concentrations of heavy metals detected in each Bio-Vase product ("Product") and heavy metals released by each Bio-Vase product after 7 days from the beginning of the experiment ("Surnatant Time 1") and after 12 days from the beginning of the experiment ("Surnatant Time 2"). The red asterisks indicate metal concentrations above the threshold value (L1 limit) of the Italian decree 173/2016.

The results of heavy metals' adsorption showed that almost all the added Cu and Pb were adsorbed by all the three IDRABEL products (on average, 96.5%). High adsorption values were also observed for Fe and Zn by the PRE-BIOFIX and by the ANAEROBIC products (on average 94.3%), unlike the AEROBIC product, which showed a 3 times lower adsorption capacity. Similar

trend was also observed for Ni and Mn, adsorbed for approximately 35% by the PRE-BIOFIX and by the ANAEROBIC products, and only for 17% and 0% by the AEROBIC product (Figure 18). Overall, these tests indicate a good potential for the IDRABEL products to immobilize heavy metals and suggest that the inorganic substrates (not the biofixed microbes) are responsible for this ability. An optimized formulation should be discussed and finalized for the scale-up of the *in-situ* bioremediation, by selecting inorganic substrates with lower contents of metals to be used for the IDRABEL products, also avoiding the addition of metals (such as Mn and Zn) as microbial stimulants.

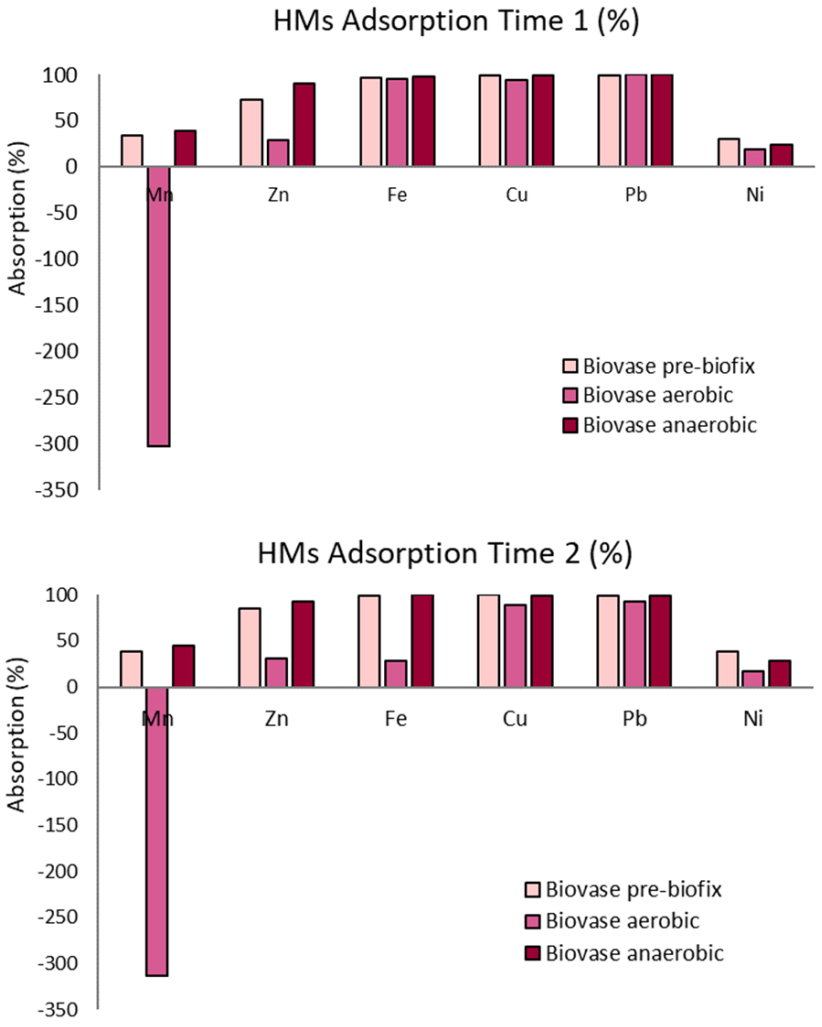

Figure 18. Heavy metals' adsorption, expressed as %, by the three Bio-Vase products the two different times. Time 1: after 7 days from the beginning of the experiment; Time 2: after 12 days from the beginning of the experiment.

3.4.2 Mesocosms

Six mesocosms (40 cm x 80 cm x 40 cm) have been setup and operated by IDRABEL to test the effect of asymmetric electric pulsing (EKOGRID technology), alone or in combination with the IDRABEL product amendment, on remediation performance. Operational parameters and monitoring results from mesocosms are reported in deliverable B.1. (Ex situ bioremediation and prototype implementation).

Similar to field monitoring tools the following methods were applied:

- GC-MS fingerprinting and diagnostic ratios
- Metabolite analysis
- BACTRAPS

In a nutshell, only weak evidence of degradation of pollutants was provided with either of these methods. At least, the decrease of total PAH in mesocosms continuously treated by the EKOGRID technology showed some evidence for enhanced attenuation after eight weeks of operation. Moreover, several BACTRAPS indicated the appearance of natural attenuation.

However, the implemented mesocosms seemed to exhibit significant artifacts, when compared to the natural environment such as:

- oxic conditions by air access (not comparable to anoxic conditions already occurring below few cm depths below the seafloor)
- loss of sediment stratification by mixing
- local inhibition/death of microbes by chlorine formation (close to titanium electrodes)
- alteration of natural conditions due to long-term operation in a closed system
- addition of Atlantic or artificial seawater instead of Mediterranean seawater
- static vs dynamic hydrodynamic conditions
- room temperature vs. variable temperature regimes.

Considering these aspects, the setup of laboratory mesocosms might not meet the practical requirements for an effective technological assessment within the SEDREMED context. Finally, the pilot field test will show the feasibility of the mesocosm approach.

3.5 Monitoring the ecosystem benefits and ecological sustainability of the applied in situ technologies

Here the results on meiofaunal and macrofaunal abundances and their taxonomic composition and organic matter quantity and biochemical composition on sediment samples collected in the different sampling areas in June, July and September 2023 before the installation of the selected

remediation technologies are provided. Data of extracellular enzymatic activities will be reported in the Deliverable 3.2 when also data dealing with the *post* treatment phase will be available.

3.5.1 Patterns of meiofauna abundance and diversity

In all sampling periods, meiofaunal abundances were variable among the different areas investigated (treatment area TR1 and TR2, artifact control and control areas; Figure 19). Besides such variability, values of meiofaunal abundances fall within the range encountered in other unpolluted benthic coastal areas worldwide (Danovaro et al., 2000; Danovaro et al., 2004; Gambi et al., 2009; Pusceddu et al., 2011; Pusceddu et al., 2014), suggesting a high level of tolerance or resilience of such a benthic component (Zeppilli et al., 2015) and/or a reduced bioavailability of contaminants (Gambi et al., 2020), despite the severe contamination of the investigated area.

Contaminants by affecting the more sensitive taxa can also influence meiofaunal biodiversity (Danovaro et al., 2009; Zeppilli et al., 2015). The analysis of meiofaunal taxa richness, indeed, revealed low values of taxa richness, suggesting an overall “poor/moderate environmental quality” of the investigated Bagnoli areas (environmental status classification based on the number of meiofaunal taxa (Danovaro et al., 2004). Independently from the areas investigated and sampling periods, the meiofaunal assemblages were almost exclusively represented by more tolerant taxa (Danovaro et al., 2009; Gambi et al., 2020) such as nematodes Figure 20), which typically are not so dominant in unpolluted benthic coastal areas (Danovaro et al., 2000; Pusceddu et al., 2011)

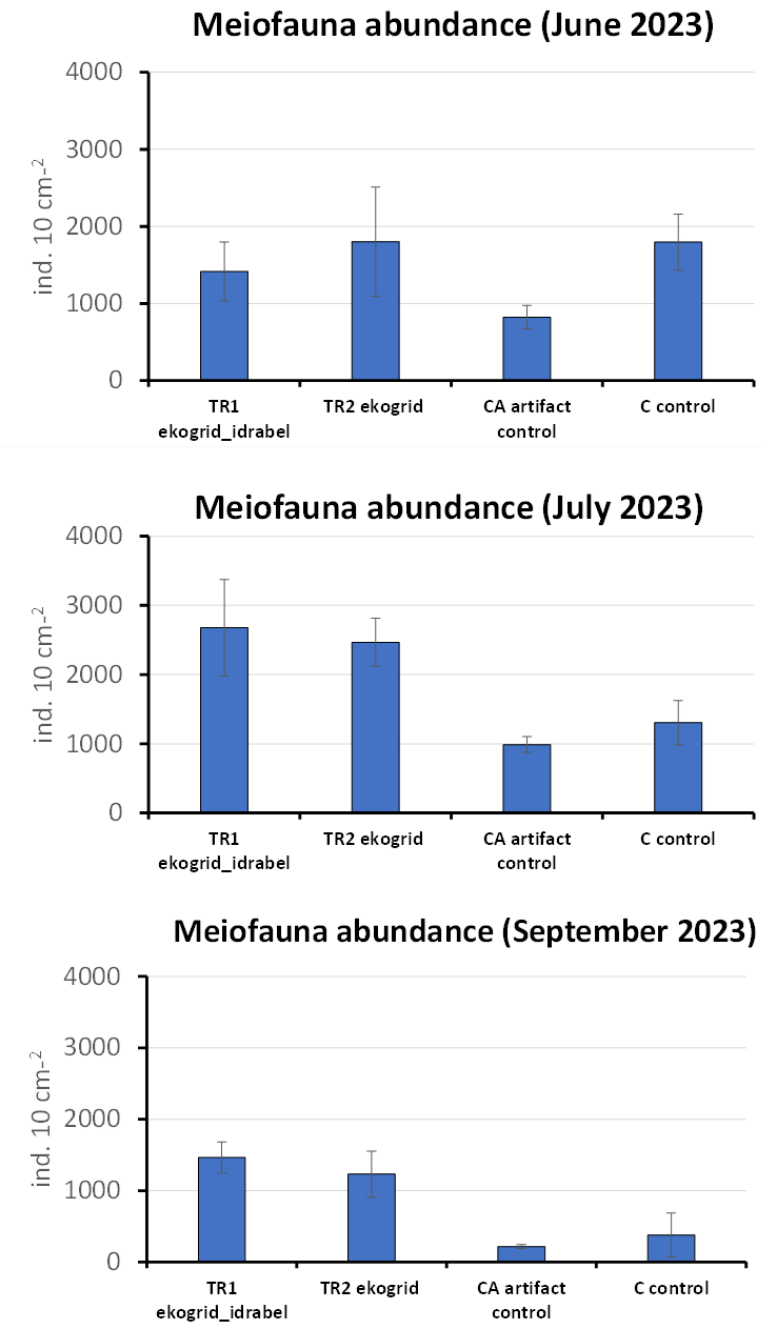

Figure 19. Meiofauna total abundance (average± standard error) determined in June, July and September 2023 in the different areas: TR1- the area in which Ekogrid and Idrabel technologies will be tested in combination); TR2 – the area in which only the Ekogrid technology will be tested; CA - the adjacent area in which the same operation for the installation of the in situ technologies will be done (i.e. artifact control); C – control area.

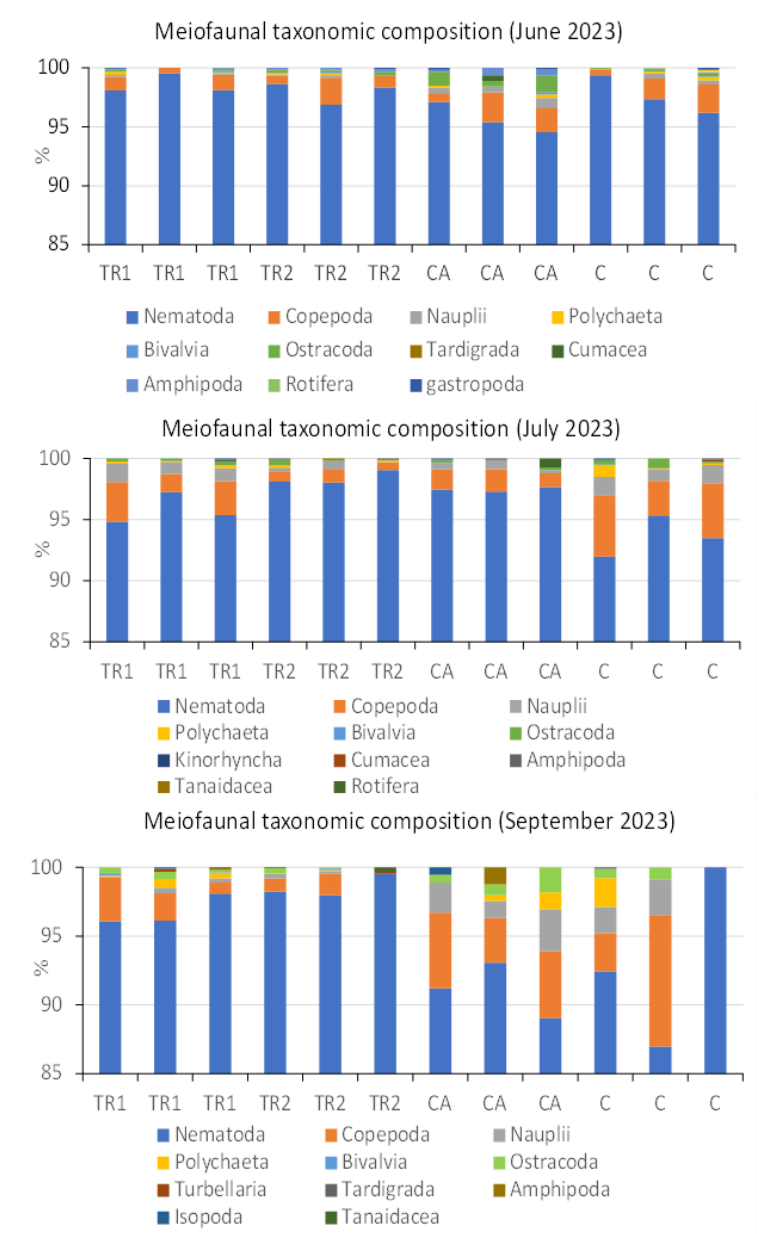

Figure 20. Taxonomic composition of meiofauna assemblages of replicate sediment samples collected in June, July and September 2023 in the different areas: TR1- the area in which Ekogrid and Idrabel technologies will be tested in combination); TR2 – the area in which only the Ekogrid technology will be tested; CA - the adjacent area in which the same operation for the installation of the in situ technologies will be done (i.e. artifact control); C – control area.

The nMDS analysis highlighted a higher dissimilarity of meiofaunal assemblage composition in September (T_2) when compared to June (T_0) and July (T_1; Figure 21).

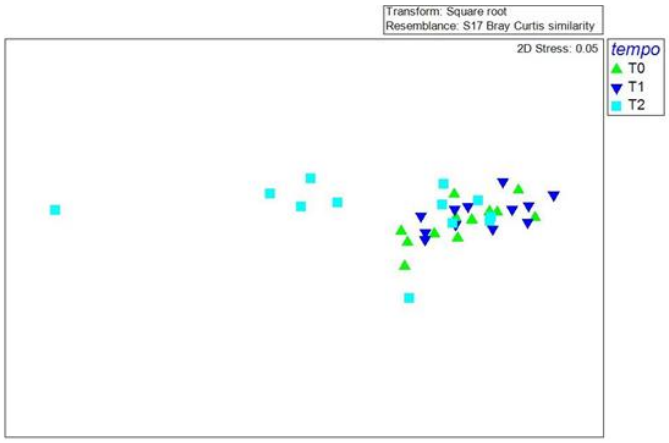

Figure 21. Output of nMDS analysis of meiofaunal assemblage composition, highlighting the factor "time".

Multivariate permutation analysis of the variance (i.e., PERMANOVA analysis) revealed the interaction "treatment × time" as significant (Table 7).

Table 7. Output of the PERMANOVA analysis performed on meiofaunal assemblage composition.

Source	df	SS	MS	Pseudo-F	P(perm)	P(MC)
treatment	3	3928.1	1309.4	2.0196	0.0829	0.1074
time	2	3792.5	1896.2	5.786	0.0004	0.0001
treatment x time	6	3890	648.33	1.9783	0.0153	0.03

					0 1
Res	2 4	78 65 .4	32 7. 73		
Total	3 5	19 47 6			

3.5.2 Organic matter quantity and biochemical composition

In all three sampling times total phytopigments concentrations were higher in areas TR1 and TR2, than in areas CA and C (Figure 22). Protein concentrations were rather constant in July 2023 and September 2023 and more variable values in June 2023 (Figure 23). Carbohydrates were the most relevant biochemical compounds of organic matter and displayed temporal variations with the highest values in June and the lowest in September 2023 (Figure 24). Lipids did not show any particular trend (Figure 25). In June 2023, biopolymeric carbon concentrations ranged from 0.8± 0.05 to 1.28± 0.08 mg g^{-1} (in the C and TR1 area, respectively). In July 2023, biopolymeric carbon concentrations displayed, on average, a limited variation (from 0.81± 0.03 mg g^{-1} to 0.97± 0.04 mg g^{-1}; Figure 26). In September 2023, biopolymeric carbon concentrations varied from 0.58± 0.03 to 0.8± 0.03 mg g^{-1} in C and TR1 areas, respectively. Based on protein and carbohydrate concentrations we found, the investigated Bagnoli areas can be classified as meso-oligotrophic (Dell'Anno et al., 2002).

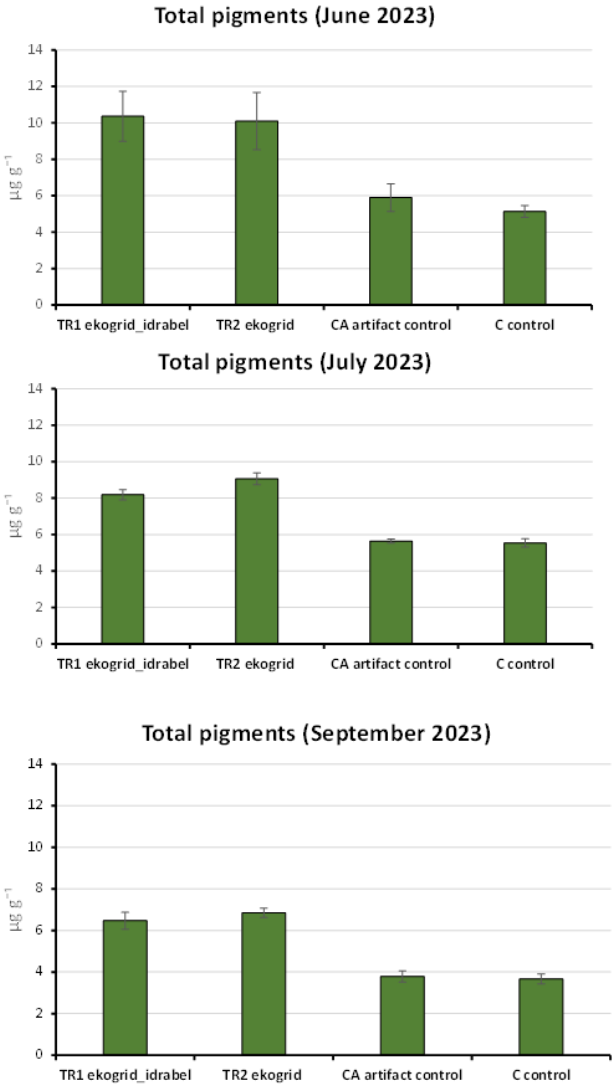

Figure 22. Total phytopigment concentrations (average ± standard error) determined in June, July and September 2023 in the different areas: TR1- the area in which Ekogrid and Idrabel technologies will be tested in combination); TR2 – the area in which only the Ekogrid technology will be tested; CA - the adjacent area in which the same operation for the installation of the in situ technologies will be done (i.e. artifact control); C – control area.

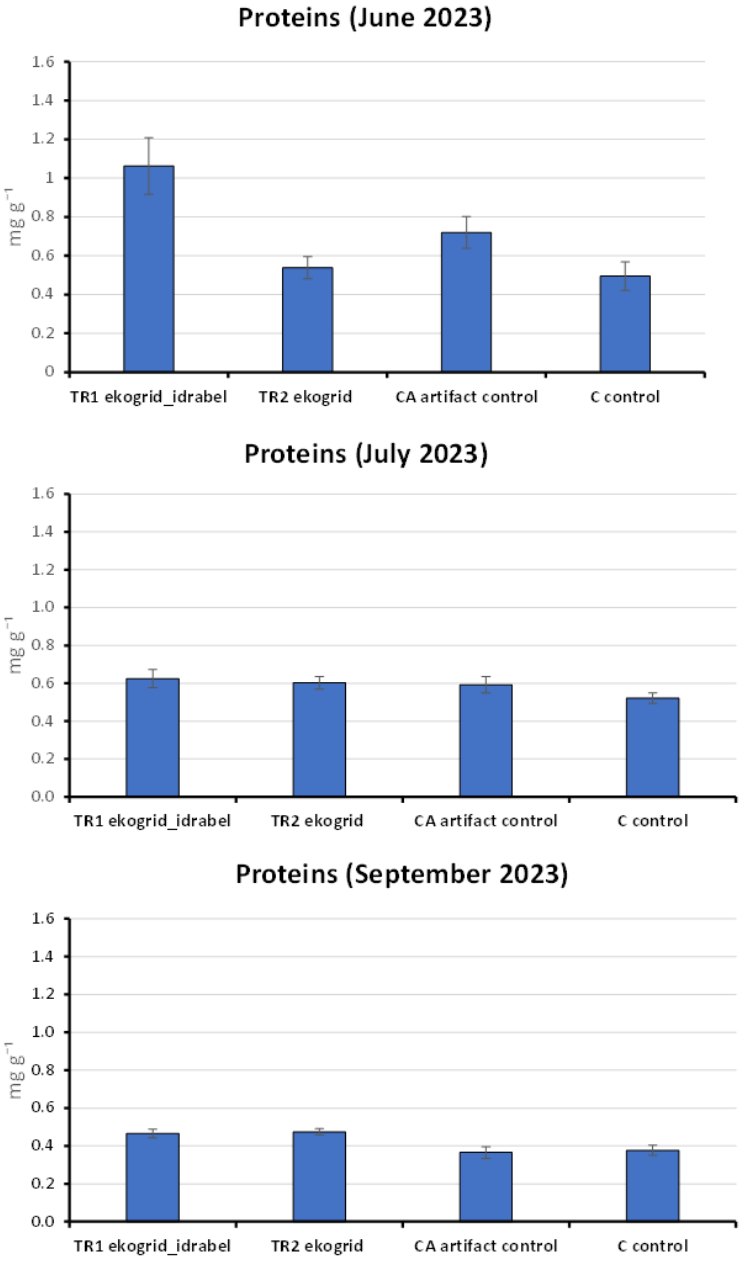

Figure 23. Protein concentrations (average± standard error) determined in June, July and September 2023 in the different areas: TR1- the area in which Ekogrid and Idrabel technologies will be tested in combination); TR2 – the area in which only the Ekogrid technology will be tested; CA - the adjacent area in which the same operation for the installation of the in situ technologies will be done (i.e. artifact control); C – control area.

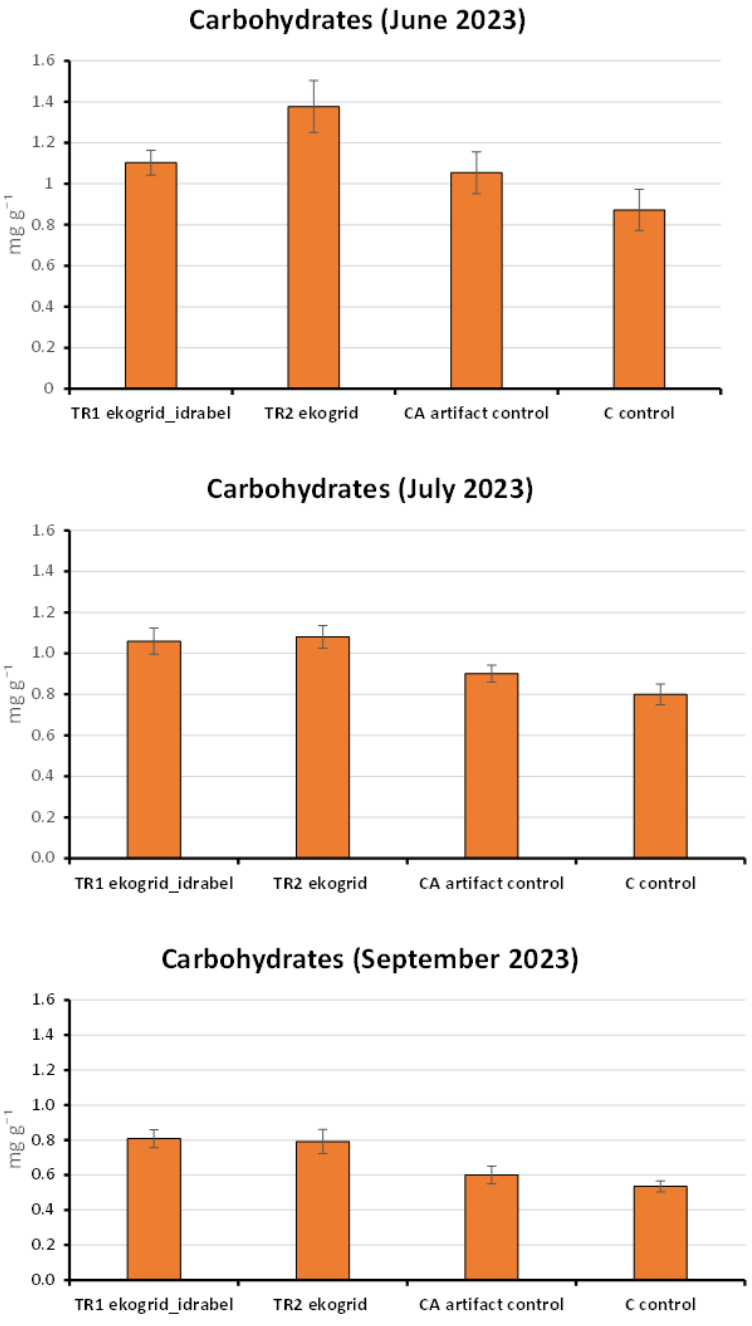

Figure 24. Carbohydrate concentrations (average± standard error) determined in June, July and September 2023 in the different areas: TR1- the area in which Ekogrid and Idrabel technologies will be tested in combination); TR2 – the area in which only the Ekogrid technology will be tested; CA - the adjacent area in which the same operation for the installation of the in-situ technologies will be done (i.e. artifact control); C – control area.

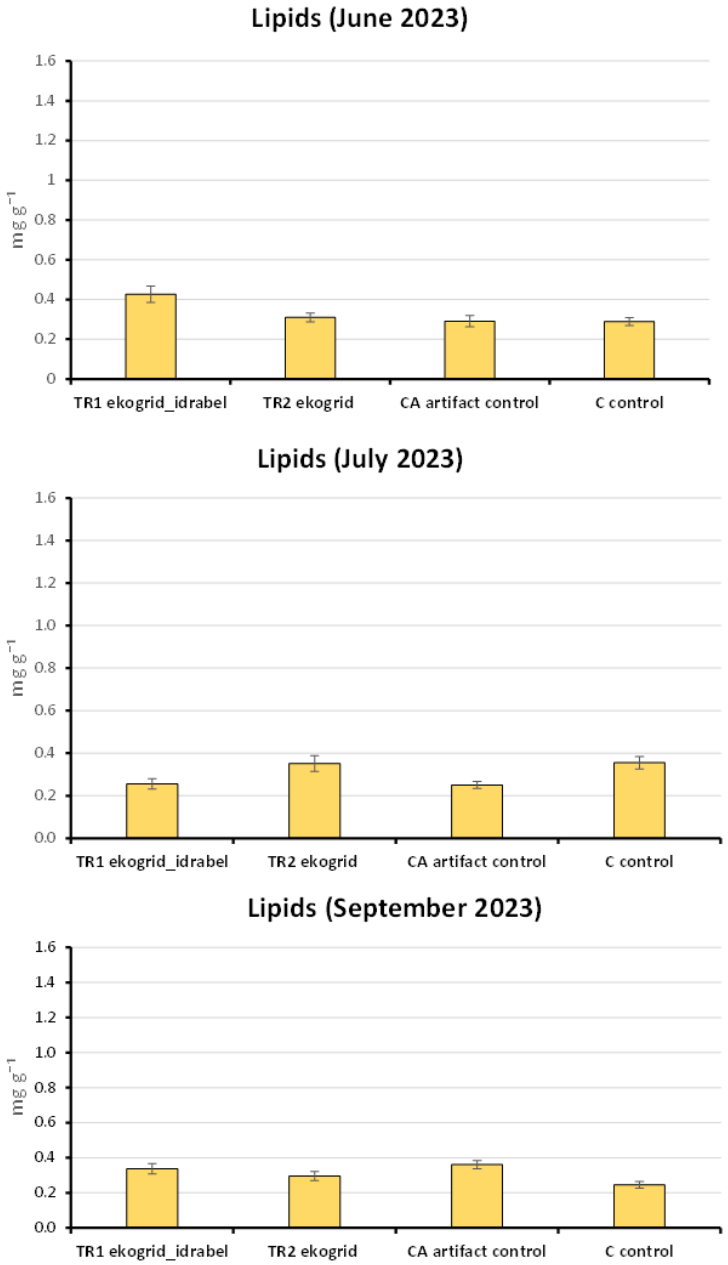

Figure 25. Lipid concentrations (average± standard error) determined in June, July and September 2023 in the different areas: TR1- the area in which Ekogrid and Idrabel technologies will be tested in combination); TR2 – the area in which only the Ekogrid technology will be tested; CA - the adjacent area in which the same operation for the installation of the in situ technologies will be done (i.e. artifact control); C – control area.

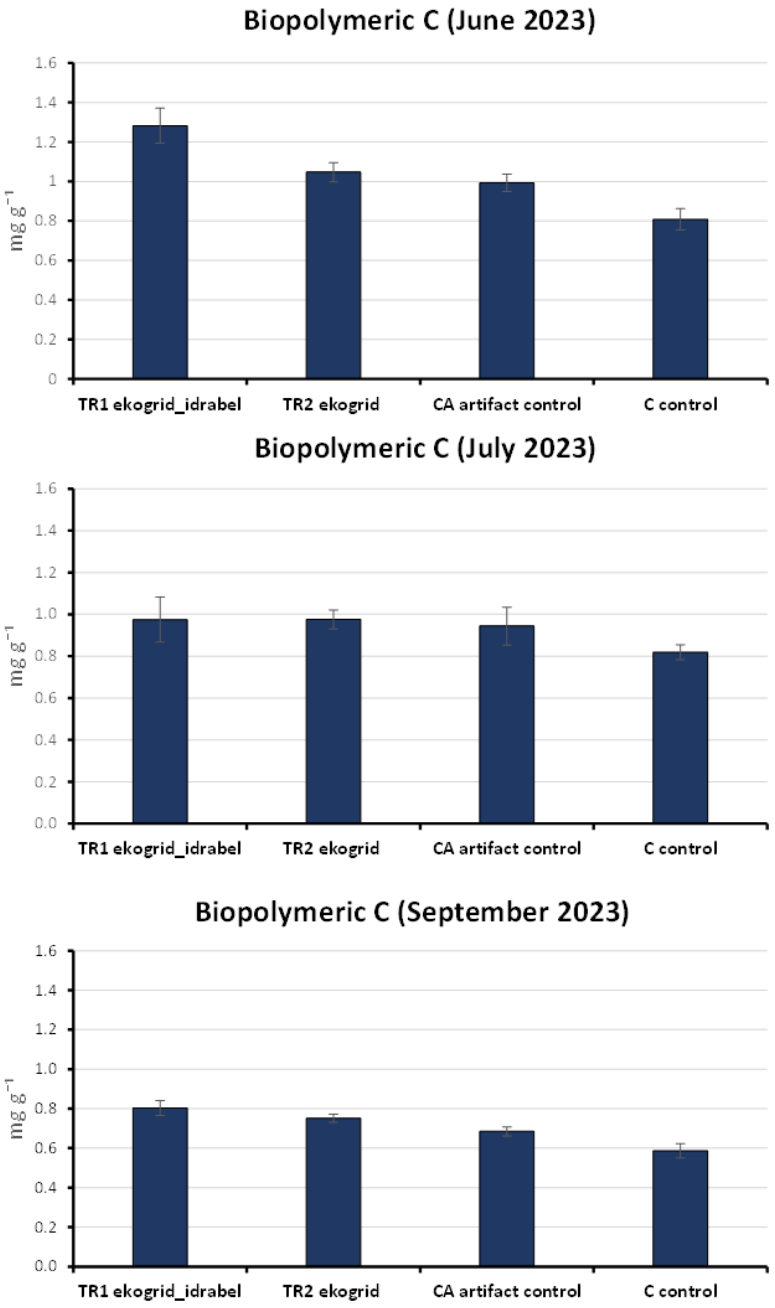

Figure 26. Biopolymeric carbon concentrations (average ± standard error) determined in June, July and September 2023 in the different areas: TR1- the area in which Ekogrid and Idrabel technologies will be tested in combination); TR2 – the area in which only the Ekogrid technology will be tested; CA - the adjacent area in which the same operation for the installation of the in-situ technologies will be done (i.e. artifact control); C – control area.

3.5.3 Patterns of macrofauna abundance and diversity

To evaluate eventual differences in the temporal patterns of the macrofaunal assemblage structure, diversity and evenness among the different areas, multivariate and univariate analyses were used. Multivariate permutational analysis of variance (PERMANOVA) used Bray–Curtis similarity matrices of abundance of taxa with 9999 permutations of residuals under a reduced model or using Monte Carlo random draws from the asymptotic permutation distribution when too few permutations were available for a given test. Homogeneity of multivariate dispersions for the interaction terms was verified with PERMDISP analysis. Non-metric multidimensional scaling (nMDS) based on centroids was used as a graphical ordination of the data. Species number (S), total abundance (N), Margalef's diversity index (d), and Pielou's evenness index (J') calculated with the DIVERSE routine on untransformed data were analyzed by means of PERMANOVAs on Euclidean distances, including the same factors described for the multivariate analysis. All multivariate tests and univariate PERMANOVA were run in the software package PRIMER-E v7 with the PERMANOVA extension.

M-AMBI values were obtained using the AMBI Software (version 6.0), which can be downloaded from the freeware http://ambi.azti.es and using the updated species list. M-AMBI integrates the Shannon-Wiener H' diversity index, the number of species (S) and the AMBI biotic index.

A total of 4283 macrofauna individuals belonging to 117 taxa were collected. The majority of the individuals were identified at species level. Among phyla, Annelida ranked first in terms of abundance with 1613 individuals, followed by Crustacea and Mollusca with 1415 and 1245 respectively, other phyla including Phoronida and Echinodermata were recorded with few individuals. Annelida ranked first also considering the number of taxa, 54, mostly identified at species level, followed by Mollusca and Crustacea with 31 and 28 taxa respectively.

The number of species was significantly variable both among treatments (ANOVA, pseudo-$F_{3,6}$ 5.0996, p = 0.0426) and sampling times (ANOVA, pseudo-$F_{2,24}$ 7.4112, p = 0.0032), being the highest at TR2 during Time 2 and the lowest at C during Time 3 (Figure 27). The abundance (number of individuals) varied with time (ANOVA, pseudo-$F_{2,24}$ 7.5716, p = 0.0032), but no differences among treatments was observed (ANOVA, pseudo-$F_{3,6}$ 1.7298, p = 0.2519) albeit resulting particularly low at C during Time 3 (Figure 28).

The Margalef's index varied similarly as the number of species being significantly variable both among treatments (ANOVA, pseudo-$F_{3,6}$ 5.3306, p = 0.0474) and sampling times (ANOVA, pseudo$F_{2,24}$ 3.991, p = 0.03), being the highest at TR2 during Time 2 and the lowest at C during Time 3 (Figure 28). Pielou's eveness varied among treatments and sampling times without a clear patter as revealed by the significance of the interaction term time×treatment (ANOVA, pseudo-$F_{3,6}$ 4.9009, p = 0.0024), being always relatively high and the highest at C during time 3 (Figure 27).

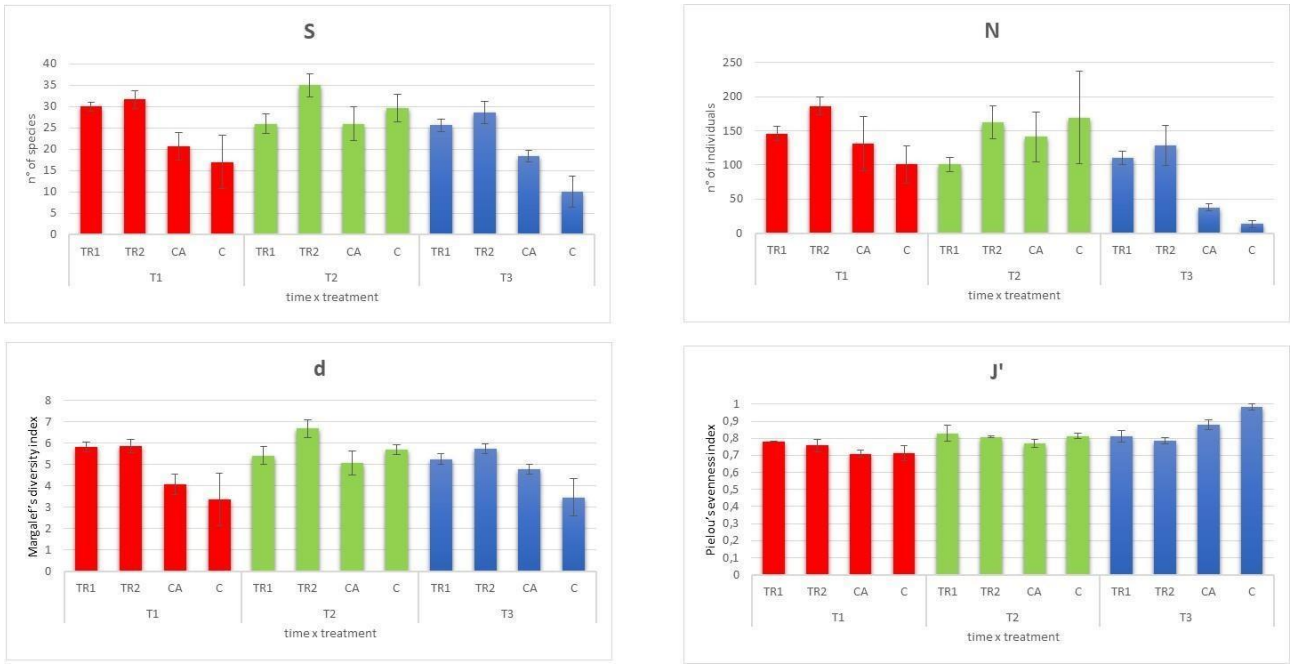

Figure 27. Variation of number of species (S), number of individuals (N), Margalef's diversity index (d) and Pielou's evenness of macrofauna assemblages among treatments (areas) and sampling times in June, July and September 2023: TR1- the area in which Ekogrid and Idrabel technologies will be tested in combination); TR2 – the area in which only the Ekogrid technology will be tested; CA - the adjacent area in which the same operation for the installation of the in situ technologies will be done (i.e. artifact control); C – control area.

As far as the multivariate assemblages is concerned the PERMANOVA revealed high variation among treatments and sampling times without a clear patter as revealed by the significance of the interaction term time×treatment (PERMANOVA, pseudo-$F_{3,6}$ 1.9878, p = 0.0001).

The nMDS output (Figure 28) based on the replicates' centroids showing the similarity (Bray-Curtis) among treatments during time, revealed the evolution of the assemblages with those sampled during time 1 being more similar to each other, whilst similarity among treatments decreased during time 3.

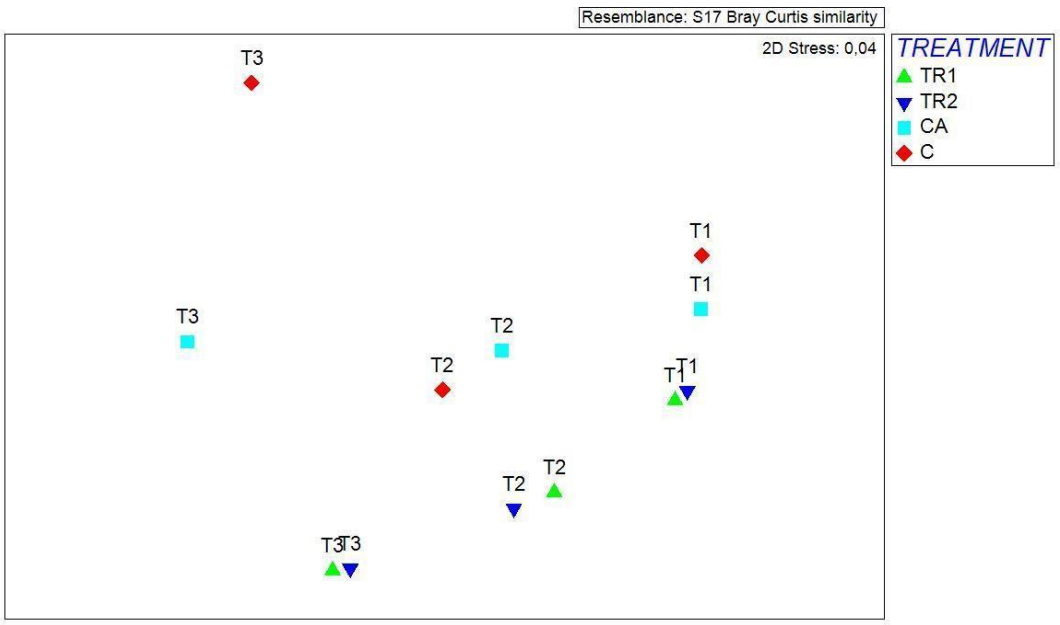

Figure 28. nMDS output showing the similarity among assemblages of the four treatments during the 3 sampling times in June, July and September 2023: TR1- the area in which Ekogrid and Idrabel technologies will be tested in combination); TR2 – the area in which only the Ekogrid technology will be tested; CA - the adjacent area in which the same operation for the installation of the in situ technologies will be done (i.e. artifact control); C – control area.

The AMBI outputs revealed that the sampled benthic assemblages were undisturbed to slightly disturbed. In particular, the majority of the species belonged to the groups 1, 2 and 3 including species sensitive to disturbance, whilst the species of the two more tolerant groups (4 and 5) were scarce (Figures 29 and Figure 30).

The M-AMBI index (Figure 31), integrating the Shannon-Wiener H' diversity index, the number of species (S) and the AMBI biotic index, revealed a generally high Ecological Quality Ratio (EQR) apart for the C treatment at time 1 resulting good albeit very close to high. Overall, these results confirm what already observed in the Bagnoli area within the ABBACO project (Musco et al., 2020).

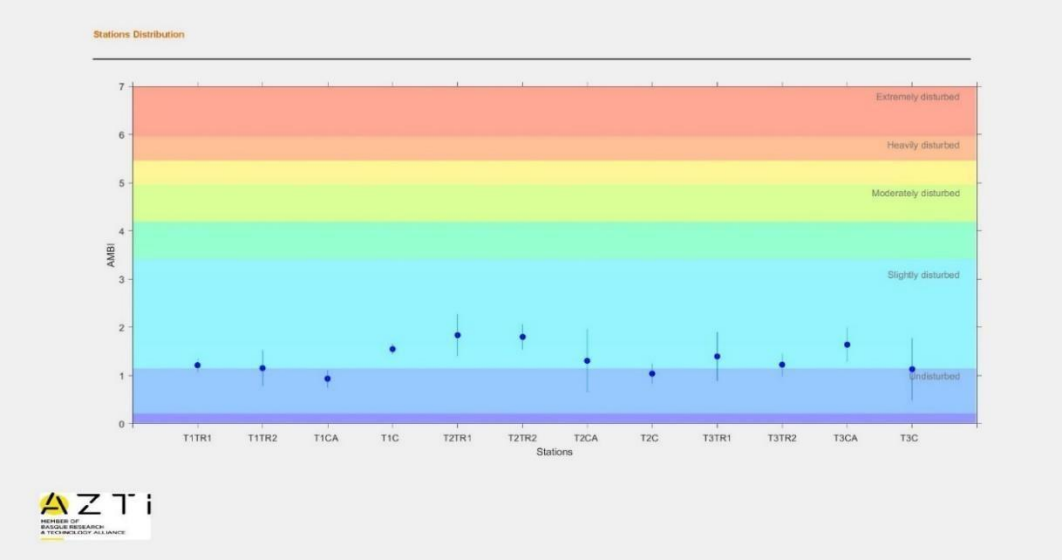

Figure 29. Average AMBI values and their variation among treatments during the 3 sampling times in June (T1), July (T2) and September (T3) 2023: TR1- the area in which Ekogrid and Idrabel technologies will be tested in combination); TR2 – the area in which only the Ekogrid technology will be tested; CA - the adjacent area in which the same operation for the installation of the in situ technologies will be done (i.e. artifact control); C – control area.

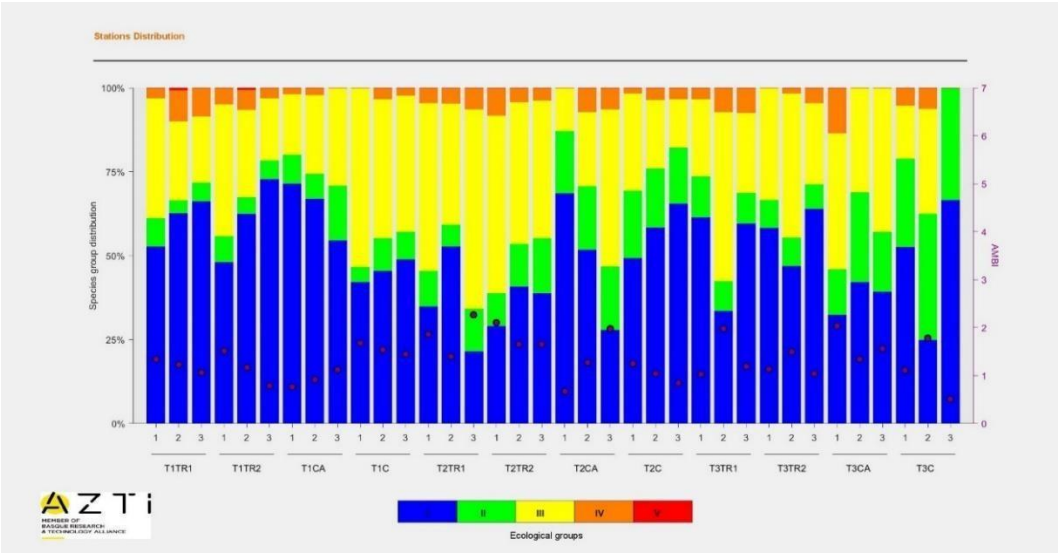

Figure 30. Relative abundance of the ecological groups to which the sampled specimens of the sampled macrofaunal assemblages were assigned per each replicate of the four treatments during the 3 sampling times in June (T1), July (T2) and September (T3) 2023: TR1- the area in which Ekogrid and Idrabel technologies will be tested in combination); TR2 – the area in which only the Ekogrid technology will be tested; CA - the adjacent area in which the same operation for the installation of the in situ technologies will be done (i.e. artifact control); C – control area.

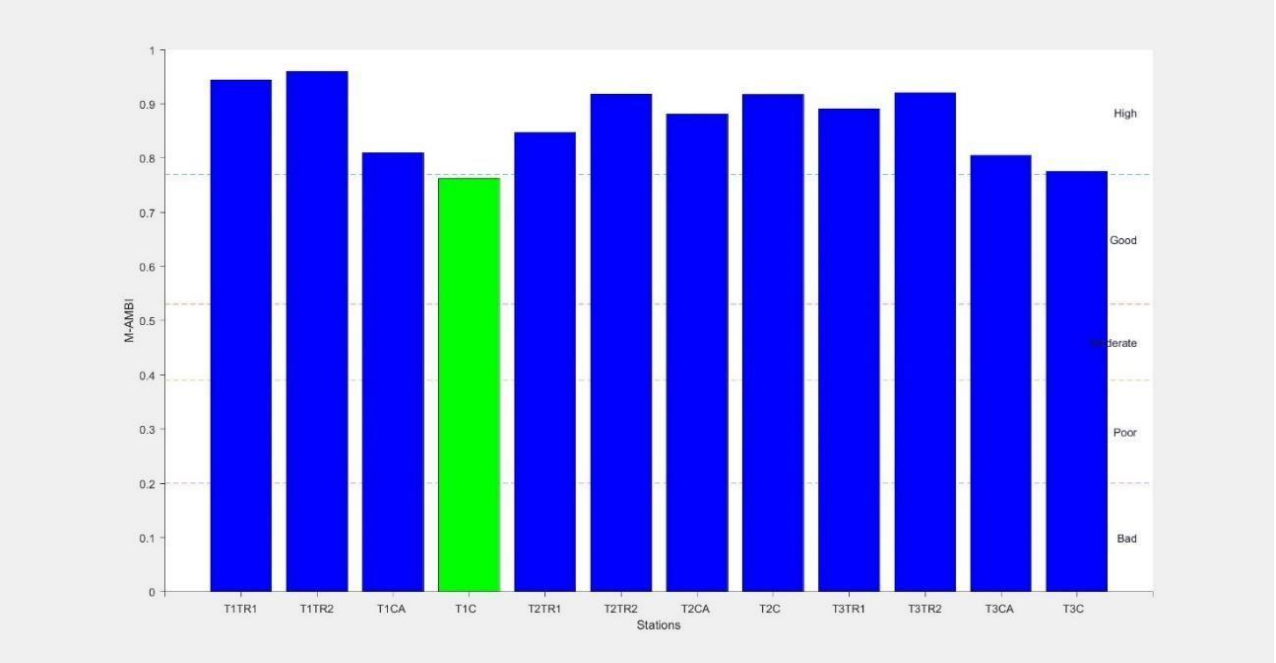

Figure 31. M-AMBI values of the macrofaunal assemblages of the four treatments during the 3 sampling times in June (T1), July (T2) and September (T3) 2023: TR1- the area in which Ekogrid and Idrabel technologies will be tested in combination); TR2 – the area in which only the Ekogrid technology will be tested; CA - the adjacent area in which the same operation for the installation of the in-situ technologies will be done (i.e. artifact control); C – control area.

4. Summary and conclusions

4.1 Monitoring results to assess and improve remediation technologies

Several monitoring methods have been successfully applied on Bagnoli sediments to provide a robust baseline for assessing remediation effects induced by the application of the proposed SEDREMED technologies (Table 8). Hereby, *in-situ* natural attenuation of polyaromatic compounds, albeit very low, has been indicated by BACTRAPS and metabolites. According to the highly differential monitoring tools and their diverse sensitivity and selectivity, multiple lines of evidence could be delivered for causal relationships for aerobic/anaerobic degradation of diluted/sorbed contaminants.

Laboratory mesocosms demonstrated that the autochthonous microbial assemblages of the Bagnoli sediments, if properly stimulated through the supply of proper electron acceptors (i.e., oxygen), can degrade to a large extent dissolved PAHs in a relatively short time scale, even till their complete mineralization. This could be achieved by in-situ supply of oxygen which can be generated by the EKOGRID technology. The amendment of the Bio-Vase product from IDRABEL, however, only slightly increased biodegradation of PAHs and might even limit PAH degradation

in a primary period of application due to elevated oxygen consumption. On the other hand, Bio-Vase is assumed to adsorb/immobilize heavy metals, which we verified by preliminary laboratory tests (Figure 18).

This preliminary observation will be experimentally assessed *in-situ* by quantifying the amount of heavy metals potentially adsorbed to the IDRABEL products during the running of the pilot field tests within the next months. Besides PAHs and heavy metals, we showed that also heavy hydrocarbons (C>12) and PCBs are relevant contaminants in the sediments of the experimental field area. Thus, the next sampling campaigns, scheduled during the running of the pilot test, will aim to verify, for the first time, the ability of the EKOGRID and IDRABEL technology in the remediation of marine sediments that display mixed contamination by PAHs, heavy metals, C>12 and PCBs.

Finally, monitoring results obtained by mesocosm experiments, carried out to assess the remediation efficiency of the EKOGRID technology alone or in combination with the IDRABEL product, provided unclear results, which currently preclude the possibility to draw definitive conclusions on the bioremediation performance of the tested technologies. These tests led to some improvements in the EKOGRID technology (e.g. implementation of steel electrodes, continuous & long-term EKOGRID application), however, further optimization and a longer running time would be needed to show significant remediation effects. As the setup and the operation of the mesocosms in the laboratory might create severe artefact conditions and it does not mirror real conditions in the field, we expect to have more definitive evidence by the ongoing pilot field test, which will allow to achieve further important insights for the effective final remediation. Once finalized, the sediment samples obtained by the pilot field tests, including control samples and samples treated by the EKOGRID technology or by the combination of EKOGRID and IDRABEL technologies, as well as BACTRAP samples, will be analyzed to monitor the efficiency of the bioremediation treatments in the study area (Table 8).

As a further insight to monitor the bioremediation potential of the microbial assemblages (especially bacteria and fungi) in the sediments, and to understand if the EKOGRID and IDRABEL treatments could allow to boost such bioremediation potential, the sediment samples already collected and those to be collected in the pilot field area will be analysed by quantitative PCR for the detection of ribosomal genes and functional genes related to PAH degradation.

Table 8. Evidence provided by chemical and microbial monitoring tools for natural or stimulated attenuation processes, respectively, in mesocosms and pilot field tests in Bagnoli regarding also certain tool features (validity, sensitivity). Classification of evidence: (-) zero, (+) minor, (++) medium, (+++) high.

Indicated		Tool						
Pollutants		Metabolites	GCMS Conc	Ratios	BACTRAPS	Lab Assays	qPCR on ribosomal genes	qPCR on functional genes
Mesocosms	Natural	-	-	-	+		march 2025	march 2025
	Stimulated	(-)	+	-	+		march 2025	march 2025
Pilot Field	Natural	+		-	+	+++	march 2025	march 2025
	Stimulated	march 2025	march 2025	march 2025	march 2025	march 2025	march 2025	march 2025
Sensitivity		medium	low	medium	high	high	high	high
Selectivity		medium	medium	medium	high	high	low	medium

The applied monitoring tools are an essential corner stone not only for the preparation, but also for the successful control of the applied remediation technologies. They provide important information on natural/stimulated degradation processes as well as site conditions so that a conceptual strategy for cost-and eco-sustainable effective remediation can be developed and optimized in a stepwise procedure (e.g. by testing in microcosm, mesocosm and field applications).

Another integral part of the monitoring campaign is the assessment of biodiversity and ecosystem health, which could be improved through remediation. Overall, the macrofaunal assemblages confirmed what observed during previous studies in the area, indicating that the first layer of the soft bottom of the Bagnoli area (the first 10 cm) were less affected by the historical impact of pollutants being thus suitable to host a diversified fauna including also sensitive species.

4.2 Improved conceptual site model and perspectives for remediation

Intense previous investigations have already shown complex and challenging contamination patterns in the Bagnoli area. However, the current investigations provided valuable insights on important factors such as contaminant sorption, redox conditions, pollutant distribution and natural attenuation processes. They can be focused on a few, short statements with strategic perspectives for remediation.

Dissolved vs. adsorbed contaminants: adsorbed contaminants on mineral particles of sediments are almost inaccessible for microbial attack and degradation in contrast to dissolved contaminants. Thus, adequate remediation strategies could also consider tools for improving contaminant desorption from the sediment matrix.

Aerobic vs. anaerobic conditions: aerobic conditions would enhance microbial degradation so that oxidation processes should be exerted in the sediment. Thus, electrochemical stimulation can be a promising approach.

Spatial distribution of pollutants: Concentrations and typologies of contaminants are high variable at relatively small spatial scale (few meters apart) and along the sediment profile. This aspect should be carefully considered for planning in situ effective and sustainable remediation strategies.

Natural attenuation vs. stimulation: Natural attenuation seems to take place in Bagnoli sediments, albeit at very low intensity. Thus, good starting conditions for the enhancement of degradation are given. Nevertheless, too much time would be necessary to achieve a final clean-up without any stimulation tool.

In-situ remediation vs. dredging: Dredging operations by inducing sediment resuspension can mobilize adsorbed contaminants, thus representing a major ecological concern. Although dredging can eliminate contaminated sediments in a relatively short time scale, dredged material needed to be properly treated or stored in disposal facilities which increase the overall management costs. Compared to that, in-situ remediation takes a long time, but it can reduce environmental risks and can be more cost effective. Particularly, the results of SEDREMED technologies could offer a promising solution for facing in a cost effective and eco-sustainable way sediment remediation in the Bagnoli area.

5. References

Akcil, A., Erust, C., Ozdemiroglu, S., Fonti, V., Beolchini, F., 2015. A review of approaches and techniques used in aquatic contaminated sediments: metal removal and stabilization by chemical and biotechnological processes. J. Clean. Prod. 86, 24–36.

Armiento, G., Caprioli, R., Cerbone, A., Chiavarini, S., Crovato, C., De Cassan, M., et al. (2020). Current status of coastal sediments contamination in the former industrial area of Bagnoli-Coroglio (Naples, Italy). Chem. Ecol. 36, 579–597.

Atlas, R., Bragg, J., 2009. Bioremediation of marine oil spills: when and when not - the Exxon Valdez experience. Microb. Biotechnol. 2, 213–221

Beolchini, F., Rocchetti, L., Regoli, F., Dell'Anno, A., 2010. Bioremediation of marine sediments contaminated by hydrocarbons: experimental analysis and kinetic modeling. J. Hazard Mater. 182, 403–407

Bianchelli S., Gambi C., Zeppilli D., Danovaro R., 2010. Metazoan meiofauna in deep-sea canyons and adjacent open slopes: A large-scale comparison with focus on the rare taxa. Deep Sea Research Part I: Oceanographic Research Papers, Volume 57, Issue 3, Pages 420-433.

Bortone, G., Arevalo, E., Deibel, I., Detzner, H.D., de Propris, L., Elskens, F., Giordano, A., Hakstege, P., Hamer, K., Harmsen, J., Hauge, A., Palumbo, L., van Veen, J., 2004. Sediment and dredged material treatment - synthesis of the SedNet work package 4 outcomes. J. Soils Sediments 4, 225–232

Budzinski, H.; Raymond, N.; Nadalig, T.; Gilewicz, M.; Garrigues, P.; Bertrand, J. C.; Caumette, P.; Aerobic biodegradation of alkylated aromatic hydrocarbons by a bacterial community. Org. Geochem. 1998, 28, 337-348.

Chen, C., Liu, Q., Liu, C., Yu, J., 2017. Effect of different enrichment strategies on microbial community structure in petroleum-contaminated marine sediment in Dalian, China. Mar. Pollut. Bull. 117, 274–282

Cruz Viggi, C., Presta, E., Bellagamba, M., Kaciulis, S., Balijepalli, S.K., Zanaroli, G., Petrangeli Papini, M., Rossetti, S., Aulenta, F., 2015. The "Oil-Spill Snorkel": an innovative bioelectrochemical approach to accelerate hydrocarbons biodegradation in marine sediments. Front. Microbiol. 6, 1–11.

Cruz Viggi, C., Matturro, B., Frascadore, E., Insogna, S., Mezzi, A., Kaciulis, S., Sherry, A., Mejeha, O.K., Head, I.M., Vaiopoulou, E., Rabaey, K., Rossetti, S., Aulenta, F., 2017. Bridging spatially segregated redox zones with a microbial electrochemical snorkel triggers biogeochemical cycles in oil-contaminated River Tyne (UK) sediments. Water Res. 127, 11–21.

Danovaro, R., Fabiano, M., 1997. Seasonal changes in quality and quantity of food available for benthic suspensionfeeders in the Golfo Marconi (North-western Mediterranean). Estuar. Coast Shelf Sci. 44 (6), 723–736.

Danovaro, R., Gambi, C., Manini, E., Fabiano, M., 2000. Meiofauna response to a dynamic river plume front. Mar. Biol. 137 (2), 359–370

Danovaro, R., Armeni, M., Dell'Anno, A., Fabiano, M., Manini, E., Marrale, D., et al., (2001). Small-scale distribution of bacteria, enzymatic activities, and organic matter in coastal sediments. Microb. Ecol. 177-185.

Danovaro, R., Gambi, C., Luna, G.M., Mirto, S., 2004. Sustainable impact of mussel farming in the Adriatic Sea (Mediterranean Sea): evidence from biochemical, microbial and meiofaunal indicators. Mar. Pollut. Bull. 49, 325– 333.

Danovaro, R., Gambi, C., Hoss, S., Mirto, S., Traunspurger, W., Zullini, A., 2009. Case studies using nematode assemblage analysis in aquatic habitats. In: Wilson, M.J., Kakouli-Duarte, T. (Eds.), Nematodes as Environmental Indicators, pp. 146–171.

Dell'Anno, A., et al., 2002. Assessing the trophic state and eutrophication of coastal marine systems: a new approach based on the biochemical composition of sediment organic matter. Mar. Pollut. Bull. 44 (7), 611–622.

Dell'Anno, A., Beolchini, F., Gabellini, M., Rocchetti, L., Pusceddu, A., Danovaro, R., 2009. Bioremediation of petroleum hydrocarbons in anoxic marine sediments: consequences on the speciation of heavy metals. Mar. Pollut. Bull. 58, 1808–1814

Dell'Anno, A., Beolchini, F., Rocchetti, L., Luna, G.M., Danovaro, R., 2012. High bacterial biodiversity increases degradation performance of hydrocarbons during bioremediation of contaminated harbor marine sediments. Environ. Pollut. 167, 85–92.

Dell'Anno, A., Beolchini, F., Corinaldesi, C., Amato, A., Becci, A., Rastelli, E., Hekeu, M., Regoli, F., Astarita, E., Greco, S., Musco, L., Danovaro, R., 2020. Assessing the efficiency and eco-sustainability of bioremediation strategies for the reclamation of highly contaminated marine sediments. Mar. Environ. Res. 162, 10510

EEA, 2019. European Bathing Water Quality in 2018

Fabiano, M., Danovaro, R., 1998. Enzymatic activity, bacterial distribution, and organic matter composition in sediments of the Ross Sea (Antarctica). Appl. Environ. Microbiol. 64, 3838–3845.

Fonti, V., Dell'Anno, A., Beolchini, F., 2015. Biogeochemical interactions in the application of biotechnological strategies to marine sediments contaminated with metals. Nov. Biotechnol. Chim. 14, 12–31.

Galperin Y., Kaplan I.R., 2008. Forensic Environmental Geochemistry in Dispute Resolution—Case History 2: Differentiating Sources of Diesel Fuel in a Plume at a Fueling Station, Environmental Forensics, 9:1, 55-62

Gambi, C., Bianchelli, S., Perez, M., Invers, O., Ruiz, J., Danovaro, R., 2009. Biodiversity response to experimental induced anoxia in seagrass sediments. Biodivers. Conserv. 18, 33–54.

Gambi, C., Dell'Anno, A., Corinaldesi, C., Lo Martire, M., Musco, L., Da Ros, Z., Armiento, G., Danovaro, R., 2020. Impact of historical contamination on meiofaunal assemblages: the case study of Bagnoli-Coroglio Bay (southern Tyrrhenian Sea). Mar. Environ. Res. 156, 10490

Haritash, A.K., Kaushik, C.P., 2016. Degradation of low molecular weight polycyclic aromatic hydrocarbons by microorganisms isolated from contaminated soil. Int. J. Environ. Sci. 6, 808–819

Head, I.M., Swannell, R.P.J., 1999. Bioremediation of petroleum hydrocarbon contaminants in marine habitats. Curr. Opin. Biotechnol. 10, 234–239

Head, I.M., Jones, D.M., Roling, W.F.M., 2006. Marine microorganisms make a meal of oil. Nat. Rev. Microbiol. 4, 173– 182.

Jacques, D., ˇSimůnek, J., Mallants, D., Van Genuchten, M.T., 2008. Modeling coupled hydrologic and chemical processes: long-term uranium transport following phosphorus fertilization. Vadose Zone J. 7, 698–711

Johnston, E.L., 2015. Chemical contaminant effects on marine ecosystem functioning. J. Appl. Ecol. 52, 140–149

Kalantary, R.R., Mohseni-Bandpi, A., Esrafili, A., Nasseri, S., Ashmagh, F.R., Jorfi, S., Jafari, M., 2014. Effectiveness of biostimulation through nutrient content on the bioremediation of phenanthrene contaminated soil. J. Environ. Heal. Sci. Eng. 12, 143.

Kowalska, J., Mazurek, R., Gasiorek, M., Zaleski, T., 2018. Pollution indices as useful tools for the comprehensive evaluation of the degree of soil contamination- a review. Environ. Geochem. Health. 40, 2395–2420.

Kronenberg, M., Trably, E., Bernet, N., Patureau, D., 2017. Biodegradation of polycyclic aromatic hydrocarbons: using microbial bioelectrochemical systems to overcome an impasse. Environ. Pollut. 231, 509–523.

Lofrano, G., Libralato, G., Minetto, D., De Gisi, S., Todaro, F., Conte, B., Calabr`o, D., Quatraro, L., Notarnicola, M., 2017. In situ remediation of contaminated marine sediment: an overview. Environ. Sci. Pollut. Res. 24, 5189–5206.

Morasch, B., Hunkeler, D., Zopfi, J., Temime, B., Hohener, P., 2011. Intrinsic biodegradation potential of aromatic hydrocarbons in an alluvial aquifer e potentials and limits of signature metabolite analysis and two stable isotopebased techniques. Water Res. 45 (15), 4459e4469

Musat, F.; Galushko, A.; Jacob, J.; Widdel, F.; Kube, M.; Reinhardt, R.; Wilkes, H.; Schink, B.; Rabus, R.; Anaerobic degradation of naphthalene and 2-methylnaphthalene by strains of marine sulfate-reducing bacteria. Environ. Microbiol. 2009, 11, 209-219.

Musco L, et al (2020). Caratterizzazione ambientale dell'area marino costiera all'interno del Sito di Interesse Nazionale di Napoli Bagnoli-Coroglio. Relazione Finale. 243 pp (Prot SZN n. 2520 del 18/05/2020).

Nastro, R.A., Gambino, E., Toscanesi, M., Arienzo, M., Ferrara, L., Trifuoggi, M., 2019. Microbial fuel cells (MFCs) remediation activity of marine sediments sampled at a dismissed industrial site: what opportunities? J. Clean. Prod. 235, 1559–1566.

Pusceddu, A., et al., 1999. Seasonal and spatial changes in the sediment organic matter of a semi-enclosed marine system (W-Mediterranean Sea). Hydrobio. 397, 59–70.

Pusceddu, A., Bianchelli, S., Gambi, C., Danovaro, R., 2011. Assessment of benthic trophic status of marine coastal ecosystems: significance of meiofaunal rare taxa. Estuar. Coast Shelf Sci. 93, 420–430.

Pusceddu, A., Gambi, C., Corinaldesi, C., Scopa, M., Danovaro, R., 2014. Relationships between meiofaunal biodiversity and prokaryotic heterotrophic production in different tropical habitats and oceanic regions. PloS One 9 (3), e91056.

Rocchetti, L., Beolchini, F., Hallberg, K.B., Johnson, D.B., Dell'Anno, A., 2012. Effects of prokaryotic diversity changes on hydrocarbon degradation rates and metal partitioning during bioremediation of contaminated anoxic marine sediments. Mar. Pollut. Bull. 64, 1688–1698.

Rulkens, W., 2005. Introduction to the treatment of polluted sediments. Rev. Environ. Sci. Biotechnol. 4, 213–221.

Unerwood, A.J. (1992) - Beyond BACI: the detection of environmental impacts on populations in the real, but variable, world. J. Exp. Mar. Biol.Ecol., 161: 145-178.

Yu, K.S.H., Wong, A.H.Y., Yau, K.W.Y., Wong, Y.S., Tam, N.F.Y., 2005. Natural attenuation, biostimulation and bioaugmentation on biodegradation of polycyclic aromatic hydrocarbons (PAHs) in mangrove sediments. Mar. Pollut. Bull. 51, 1071–1077.

Yunker, M. B., Macdonald, R. W., Vingarzan, R., Mitchell, R. H., Goyette, D., & Sylvestre, S. (2002). PAHs in the Fraser River basin: a critical appraisal of PAH ratios as indicators of PAH source and composition. Organic geochemistry, 33(4), 489-515.

Wammer, K. H.; Peters, C. A.; Polycyclic aromatic hydrocarbon biodegradation rates: A structure-based study. Environ. Sci. Technol. 2005, 39, 2571-2578.

Wang, Z.; Fingas, M.; Blenkinsopp, S.; Sergy, G.; Landriault, M.; Sigouin, L.; Foght, J.; Semple, K.; Westlake, D. W. S.; Comparison of oil composition changes due to biodegradation and physical weathering in different oils. J. Chromatogr. A 1998, 809, 89-107.

Zeppilli, D., Sarrazin, J., Leduc, D., Martinez Arbizu, P., Fontaneto, D., Fontanier, C., et al., 2015. Is the meiofauna a good indicator for climate change and anthropogenic impacts? Mar. Biodivers. 45, 505–535.

6. Appendix

6.1 Manuals used for the identification of the macrofauna

Cepeda D., Lopez E., San Martin G., Parapar J. (2022) Annelida Polychaeta VI. Fauna Iberica, vol. 47, MNCN - CSIC, Madrid, Spain, 452 pp.

Doneddu M., Trainito E. (2005) Conchiglie del Mediterraneo. Ed. Il Castello, 256 pp.

Falciai L., Minervini R. (1992) Guida dei crostacei decapodi d'Europa. Franco Muzzio Editore, Padova, Italy, 318 pp.

Fauvel P. (1923) Faune de France, vol. 5. Polychètes Errantes. Paris, Paul Lechevalier, 491 pp.

Fauvel P. (1927) Faune de France, vol. 16. Polychètes Sedentaires. Paris, Paul Lechevalier, 497 pp.

Parapar J., Adarraga I., Aguado M.T., Aguirrezabalaga F., Besteiro C., Bleidorn C., Capa M., Capaccioni-Azzati R., ElHaddad M., Fernandez-Alamo M.A., Lopez E., Martinez J., Martinez-Ansemil E., Moreira J., Nunez J., Ravara A. (2018) Annelida Polychaeta V. Fauna Iberica, vol. 45, MNCN - CSIC, Madrid, Spain, 631 pp.

Parapar J., Alos C., Nunez J., Moreira J., Lopez E., Aguirrezabalaga F., Besteiro C., Martinez A. (2012) Annelida Polychaeta III. Fauna Iberica, vol. 36, MNCN - CSIC, Madrid, Spain, 413 pp.

Parapar J., Moreira J., Nunez J., Barnich R., Brito M.C., Fiege D., Capaccioni-Azzati R., El-Haddad M. (2015) Annelida Polychaeta IV. Fauna Iberica, vol. 41, MNCN - CSIC, Madrid, Spain, 413 pp.

Ruffo S. (Ed.) (1982) The Amphipoda of the Mediterranean Sea. Part 1. Memoires de l'Institut Océanographique, Fondation Albert I Prince de Monaco n. 13, pp. 1-364.

Ruffo S. (Ed.) (1989) The Amphipoda of the Mediterranean Sea. Part 2. Memoires de l'Institut Océanographique, Fondation Albert I Prince de Monaco n. 13, pp. 365-576.

Ruffo S. (Ed.) (1993) The Amphipoda of the Mediterranean Sea. Part 3. Memoires de l'Institut Océanographique, Fondation Albert I Prince de Monaco n. 13, pp. 577-813.

Ruffo S. (Ed.) (1998) The Amphipoda of the Mediterranean Sea. Part 4. Memoires de l'Institut Océanographique, Fondation Albert I Prince de Monaco n. 13, pp. 814-959.

San Martin G. (2003) Annelida Polychaeta II - Syllidae. Fauna Iberica, vol. 21, MNCN - CSIC, Madrid, Spain, 554 pp.

Tortonese E. (1965) Fauna d'Italia, vol. VI - Echinodermata. Ed. Calderini, 424 pp.

Viéitez J.M., Alos C., Parapar J., Besteiro C., Moreira J., Nunez J., Laborda A.J., San Martin G. (2004) Annelida Polychaeta I. Fauna Iberica, vol. 25, MNCN - CSIC, Madrid, Spain, 530 pp.

Zenetos A., Gofas S., Russo G.F., Templado J. (2005) CIESM Atlas of exotic species in the Mediterranean. Vol. 3. Molluscs. CIESM Publications, Monaco, 376 pp.